Title: Epigenomic profiling of primate LCLs reveals the evolutionary patterns of epigenetic activities in gene regulatory architectures

Authors: Raquel García-Pérez[1*#], Paula Esteller-Cucala[1#], Glòria Mas[2,3], Irene Lobón[1], Valerio Di Carlo[2,3], Meritxell Riera[1], Martin Kuhlwilm[1], Arcadi Navarro[1,4,5], Antoine Blancher[6,7], Luciano Di Croce[2,3,5], José Luis Gómez-Skarmeta[8], David Juan[1*#], Tomàs Marquès-Bonet[1,4,9,10*#]

Affiliations:

[1] Institute of Evolutionary Biology (UPF-CSIC), PRBB, Barcelona, Spain

[2] Centre for Genomic Regulation (CRG), The Barcelona Institute of Science and Technology, Spain

[3] Universitat Pompeu Fabra (UPF), Barcelona, Spain

[4] National Institute for Bioinformatics (INB), PRBB, Barcelona, Spain

[5] Institució Catalana de Recerca i Estudis Avançats (ICREA), Barcelona, Spain

[6] Laboratoire d'immunologie, CHU de Toulouse, Institut Fédératif de Biologie, hôpital Purpan, Toulouse, France

[7] Centre de Physiopathologie Toulouse-Purpan (CPTP), Université de Toulouse, Centre National de la Recherche Scientifique (CNRS), Institut National de la Santé et de la Recherche Médicale (Inserm), Université Paul Sabatier (UPS), Toulouse, France

[8] Centro Andaluz de Biología del Desarrollo (CABD), Consejo Superior de Investigaciones Científicas-Universidad Pablo de Olavide-Junta de Andalucía, Seville, Spain

[9] CNAG-CRG, Centre for Genomic Regulation (CRG), Barcelona Institute of Science and Technology (BIST), Barcelona, Spain

[10] Institut Català de Paleontologia Miquel Crusafont, Universitat Autònoma de Barcelona, Cerdanyola del Vallès, Barcelona, Spain

[#] Contributed equally to this work

*Corresponding author. Email: tomas.marques@upf.edu (T.M.-B); david.juan@upf.edu (D.J.); raquel.garcia@bsc.es (R.G.-P.)

Summary

To gain insight into the evolution of the epigenetic regulation of gene expression in primates, we extensively profiled a new panel of human, chimpanzee, gorilla, orangutan, and macaque lymphoblastoid cell lines (LCLs), using ChIP-seq for five histone marks, ATAC-seq and RNA-seq, further complemented with WGS and WGBS. We annotated regulatory elements and integrated chromatin contact maps to define gene regulatory architectures, creating the largest catalog of regulatory elements in primates to date. We report that epigenetic conservation and its correlation with sequence conservation in primates depends on the activity state of the regulatory element. Our gene regulatory architectures reveal the coordination of different types of components and highlight the role of promoters and intragenic enhancers in the regulation of gene expression. We observed that most regulatory changes occur in weakly active intragenic enhancers. Remarkably, novel human-specific intragenic enhancers with weak activities are enriched in human-specific mutations. These elements appear in genes with signals of positive selection, tissue-specific expression and particular functional enrichments, suggesting that the regulatory evolution of these genes may have contributed to human adaptation.

Keywords: Epigenomics, gene regulation, evolution, positive selection.

Introduction

Changes in chromatin structure and gene regulation play a crucial role in evolution[1,2]. Gene expression differences have been extensively studied in a variety of species and conditions[3–6]. However, there is still much unknown about how regulatory landscapes evolve, even in closely related species. Previous work has focused on the dynamics of the addition and removal of regulatory elements with signals of strong activity during mammalian evolution –mainly defined from ChIP-seq experiments on a few histone marks[7–10]. These analyses suggested that enhancers evolve faster than promoters[8,11]. The number of active enhancers located near a gene –its regulatory complexity –has also been reported to influence the conservation of gene expression in mammals[9].

Moreover, in a selected group of primates –mostly chimpanzees and macaques– changes in histone mark enrichments are associated with gene expression differences[12]. Several studies have also targeted the appearance of human-specific methylation patterns[13,14] and active promoters and enhancers in different anatomical structures and cell types[8,10]. All these studies have proven that comparative epigenomics is a powerful tool to investigate the evolution of regulatory elements[15,16]. However, a deeper understanding of the evolution of gene regulation requires the integration of multi-layered epigenome data. Only such integration can provide the necessary resolution of regulatory activities for investigating recent evolutionary time frames, as is the case within the primate lineage. Here, we provide an in-depth comparison of the recent evolution of gene regulatory architectures using a homologous cellular model system in human and non-human primates.

Results

Comprehensive profiling of primate lymphoblastoid cell lines (LCLs)

We have extensively characterized a panel of lymphoblastoid cell lines (LCLs) from human, chimpanzee, gorilla, orangutan, and macaque, including two independent biological replicates for each species. This characterization includes chromatin immunoprecipitation data (ChIP-seq) from five key histone modifications (H3K4me1, H3K4me3, H3K36me3, H3K27ac, and H3K27me3) and deep-transcriptome sequencing (RNA-seq) (Fig. 1). We integrate these datasets into gene regulatory architectures (Fig. 2a and Supplementary Figs. 1 and 2) to (1) understand how primate gene expression levels are controlled and how expression changes between species occur and to (2) study patterns of evolutionary conservation of regulatory elements in primates. To complement this resource, we have also processed high coverage whole-genome and whole-genome bisulfite sequencing data, as well as chromatin accessibility data (Supplementary Tables 1-10 and Additional

88 files 1-5). Taken together, this is the most extensive collection of great apes and macaque
89 transcriptomic and epigenomic data to date.

90

91 **Annotation of regulatory elements**

92 We used the signal of the ChIP-seq experiments from the five histone marks to identify regulatory
93 regions with characteristic marks of promoters or enhancers (Supplementary Figs. 1 and 2). We
94 defined regulatory regions for each cell line as those containing chromatin states (overrepresented
95 combinations of histone marks detected by ChromHMM[17]) enriched in any regulatory-related histone
96 mark (Fig. 2a and Supplementary Fig. 1). We merged overlapping regulatory regions in the two
97 replicates of every species to define species regulatory elements.

98 We classified the chromatin states of the regulatory elements based on a hierarchy of functionally
99 interpretable epigenetic states. This hierarchy differentiates chromatin states into promoter (P) and
100 enhancer (E) states, with three different levels of activity each: strong (s), poised (p), or weak (w)
101 (Methods and Supplementary Fig. 1). We improved these assignments by applying a linear
102 discriminative analysis (LDA) with normalized histone and open chromatin enrichments (Methods
103 and Supplementary Figs. 3 and 4). The refined classification results in more similar regulatory
104 landscapes between biological replicates (Wilcoxon signed rank-test: $P < 0.05$ in all species;
105 Supplementary Figs. 5 and 6), with more regulatory elements with the same state in all species
106 (Wilcoxon signed rank-test: $P = 0.03$; Supplementary Figs. 7 and 8).

107 On average, we found ~11,000 and ~76,000 regulatory elements with promoter and enhancer states
108 per species, respectively (Fig. 2b), of which 69% and 33% are strong, 8% and 4% are poised, and
109 14% and 45% are weak, respectively (Supplementary Fig. 9 and Supplementary Table 1). Strong and
110 poised activities are more associated with promoter states, whereas weak activities are more
111 frequently associated with enhancer states (Chi-square test: $P < 2.2 \times 10^{-16}$ in all species;
112 Supplementary Fig. 10). We associated regulatory elements with genes using 1D gene proximity and
113 existing high-resolution 3D chromatin contact data for one of the human LCLs (Fig. 2a and Methods).
114 On average, 70% of the regulatory elements are associated with genes, of which 93% are protein-
115 coding and 61% are 1-to-1 orthologous protein-coding genes in all primate species (Fig. 2c). The set
116 of regulatory elements associated with a gene defines its regulatory architecture.

117 Altogether, this catalog of regulatory elements provides a comprehensive view of the regulatory
118 landscape of LCLs in humans and non-human primates. In contrast to other commonly used
119 definitions of promoters and enhancers limited to strongly active regions, our multi-layered

integration approach allows the additional annotation of weak and poised activities[7,8]. These activities are of particular relevance to improve the definition of elements in regulatory gene architectures. In sum, a detailed primate regulatory catalog enables the study of the evolution of these regulatory activities using LCLs as a proxy of their regulatory potential in other cell types or conditions.

The evolutionary dynamics of promoters and enhancers in primate LCLs recapitulate previous observations in more distant mammals

Inter-species differences in regulatory regions can be associated with genomic or epigenetic changes. Inconsistencies in the quality of genome assemblies make it difficult to distinguish actual inter-species genomic differences, an issue aggravated in multi-species comparisons. To overcome this problem, we restricted our analyses to unambiguous 1-to-1 orthologs between all species. We detected 28,703 1-to-1 orthologous genomic regions in the five species with a promoter or enhancer state in at least one species (Supplementary Fig. 11). Most of these orthologous regulatory regions (~76%, Binomial test: $P < 2.2 \times 10^{-16}$) are associated with genes (Methods). In downstream analyses, we focused on these regions integrating the regulatory architectures of protein-coding and non-coding genes.

We quantified the conservation of epigenetic states in regulatory regions as the number of primate species with the epigenetic state in the orthologous regions. In the regulatory architectures of protein-coding genes, promoter states are more conserved than enhancer states (Supplementary Figs. 12-14), with 73% and 60% of regions with a promoter or enhancer state being fully conserved across primates, respectively (Fisher's exact test: $P < 2.2 \times 10^{-16}$, $OR = 1.84$; Supplementary Fig. 13). Less than 14% and 8% of orthologous regulatory regions with a promoter or enhancer state are specific to a primate species, respectively (Supplementary Fig. 13). These results for protein-coding genes fall in line with the higher conservation of promoters previously observed in mammals[7]. In contrast, for non-coding genes, promoter states are less conserved than enhancer states (Fisher's exact test: $P < 2.2 \times 10^{-16}$, $OR = 0.39$; Supplementary Fig. 14), with 46% and 69% of fully conserved and 26% and 3% of species-specific elements, respectively.

Intrigued by the different epigenetic conservation patterns in protein-coding and non-coding genes, we studied the repurposing and acquisition of regulatory elements. We defined *recently repurposed promoters* –or *enhancers*– as regulatory regions with a promoter state in only one species and enhancer states in the remaining species –or vice versa. Similarly, *recently gained promoters* or *enhancers* are those regions with a promoter or enhancer state in one species and without regulatory states in any other species.

153 In agreement with previous studies in more distant species[18], nearly all (93%) recently evolved
154 promoter states are acquired through repurposing events, whereas the majority (90%) of recently
155 evolved enhancer states are gained (Chi-square test: $P < 2.2 \times 10^{-16}$; Methods and Supplementary
156 Figs. 15 and 16). The regulatory architectures of protein-coding and non-coding genes –the latter
157 evaluated in human due to underrepresentation of non-coding gene annotations in non-human
158 species– show this same pattern (Fisher's exact test: $P < 2.2 \times 10^{-16}$, OR = Inf, and $P = 6.2 \times 10^{-16}$,
159 OR = 138 respectively; Supplementary Fig. 15).

160 Our findings confirm those in more distant species[7,18] and reinforce the generality of these
161 evolutionary dynamics in protein-coding genes. The acquisition of regulatory states in the regulatory
162 architectures of non-coding genes resembles that of protein-coding genes. However, the lower
163 conservation of promoter states associated with non-coding genes suggests that their overall higher
164 conservation is not an intrinsic characteristic of promoter states and that it depends on their specific
165 regulatory relevance in different genes.

166

167 **The activity of promoter and enhancers influences their epigenetic and sequence conservation**

168 Taking advantage of our classification of promoters and enhancers into three different activities
169 (strong, poised, and weak), we further explored the patterns of evolutionary conservation of the
170 different regulatory states. Globally, orthologous regulatory regions conserve their regulatory state
171 (Randomization analyses: 1,000 simulations, $P < 0.05$; Supplementary Figs. 17-19 and
172 Supplementary Table 11), but different promoter and enhancer activities show characteristic patterns
173 of conservation (Kruskal-Wallis test: $P < 2.2 \times 10^{-16}$; Fig. 3a and Supplementary Figs. 20-22).

174 Strong promoters are the most conserved activities: 80% of them are fully conserved in primates. On
175 the contrary, poised and weak promoters are poorly conserved (Fig. 3a). All enhancer activities show
176 a similar pattern of evolutionary conservation (Fig. 3a). Enhancer states with strong activities are
177 second in conservation after strong promoters. Nearly 40% of the orthologous regulatory regions with
178 strong enhancer states are fully conserved. Poised enhancers follow closely, with 36% of them
179 conserved in the five species. Lastly, around 21% of the regions with a weak enhancer conserve their
180 activity across primates. The regulatory regions associated with protein-coding and non-coding genes
181 show the same conservation trends (Supplementary Figs. 23 and 24). However, strong activities in
182 promoter states are less common for non-coding than for protein-coding genes, leading to lower
183 conservation of promoter compared to enhancer states. This shows that differences in activity
184 composition can lead to differences in the conservation of the regulatory architectures.

185 The epigenetic states in a given cell type and their evolutionary conservation reflect the specific
186 function of the regulatory regions in this cell type. These regions are expected to show different states
187 in other cell types and so their evolutionary patterns might also be different. To investigate whether
188 changes in activity are likely to affect the epigenetic conservation of regulatory elements, we assessed
189 the association between epigenetic and sequence conservation –which is cell type-independent. First,
190 we observed that epigenetic conservation significantly correlates with the conservation of the
191 underlying sequence –quantified as z-scores of background normalized PhastCons values[19]– in all
192 epigenetic states but weak promoter states (Fig. 3b, Methods and Supplementary Fig. 25). These
193 correlations are seen in the architectures of protein-coding but not in non-coding genes
194 (Randomization analyses: 1,000 simulations; Fig. 3b, Supplementary Figs. 26-30). Of note,
195 orthologous regulatory regions with fully conserved epigenetic states show significant differences in
196 sequence conservation (Kruskal-Wallis test: $P < 2.2 \times 10^{-16}$; Supplementary Fig. 31). In particular,
197 strong and weak promoters are associated with higher and lower sequence conservation scores
198 respectively, whereas all enhancer states range in between these values. (Dwass-Steel-Critchlow-
199 Fligner test, Supplementary Fig. 31). The sequence conservation scores associated with strong and
200 poised enhancers are not significantly different. Note also that conserved poised promoters are
201 associated with very high conservation z-scores, which probably did not reach significance due to
202 their low number (n = 9 pP). Orthologous regions associated with non-coding genes are fewer and
203 less epigenetically conserved (Supplementary Figs. 24 and 27), which could explain the lack of
204 correlation between the conservation of the sequence and the epigenetic state observed in all but
205 strong enhancers (Supplementary Fig. 30).

206 These results demonstrate that a detailed classification of promoters and enhancers with different
207 activities into regulatory architectures provides a deeper understanding of their evolutionary
208 constraints and dynamics, expanding previous observations in mammals[7] that could mostly be made
209 for active regulatory activities. The consistent association of epigenetic and sequence conservation
210 also suggests that the epigenetic conservation observed in LCLs is a good proxy for the conservation
211 of the regulatory activity of these elements in our primate species.

212

213 **Definition of different types of components in the regulatory architectures**

214 To characterize the evolution of regulatory elements based on their specific role in gene expression,
215 we classified regulatory elements into five different components according to the role they had in the
216 gene regulatory architectures (Fig. 4a, Methods). We first classified regulatory elements based on
217 their proximity to a gene into three types of components: genic promoters (gP), intragenic enhancers

218 (gE), and proximal enhancers (prE). As gene expression is controlled by a combination of short- and
219 long-distance regulatory interactions[20], we used available 3D chromatin contact maps for human
220 LCLs[21–23] to link interacting regulatory elements to their target gene/s and define two additional types
221 of components: promoter-interacting enhancers (PiE) and enhancer-interacting enhancers (EiE) (Fig.
222 4a).

223 We were able to link to genes and classify, on average, nearly 3,500 otherwise orphan distal
224 regulatory elements per species (Supplementary Fig. 32). We annotated ~12,500 genic promoters,
225 ~35,000 intragenic enhancers, ~6,700 proximal enhancers, ~6,200 promoter-interacting enhancers,
226 and ~1,800 enhancer-interacting enhancers per species (Fig. 4b and Supplementary Fig. 33), of which
227 48%, 69%, 40%, 62%, and 61% are associated with 1-to-1 orthologous protein-coding genes in all
228 primate species (Fig. 4c).

229 To assess the consistency of our classification of regulatory components, we focused on 1-to-1
230 orthologous protein-coding genes considering all their associated regulatory elements (i.e. 6
231 epigenetic states x 5 components = 30 regulatory subcategories). We found high concordance
232 between the epigenetic state (based on ChIP-seq and ATAC-seq data, Fig. 2a) and the component
233 (based on the type of association with the gene, Fig. 4a) of the regulatory elements. On average, 75%
234 of genic promoters have a promoter state, and 90% of gene-associated enhancers have an enhancer
235 state (Fisher's exact test: $P < 2.2 \times 10^{-16}$ in all species, average $OR = 64$; Supplementary Fig. 34).
236 This concordance is also consistent across species (Chi-square test: $P < 2.2 \times 10^{-16}$ in all species; Fig.
237 4d and Supplementary Fig. 35). Genic promoters are enriched in regulatory elements with strong
238 promoter and poised promoter and enhancer states. Strong enhancers are mostly enriched at intragenic
239 and promoter-interacting enhancers, whereas weak enhancers are strongly associated with proximal
240 enhancers (Supplementary Figs. 34 and 35).

241 Gene expression levels are positively associated with the presence of strong activities in their
242 regulatory architectures and are negatively associated with the presence of poised or weak activities
243 (Kruskal-Wallis test: $P < 0.05$ in all species and regulatory components; Supplementary Fig. 36).
244 These associations are particularly strong in genic promoters and intragenic enhancers (Dwass-Steel-
245 Critchlow-Fligner test; Supplementary Fig. 37). Despite the consistency between the components'
246 activities and gene expression, our results suggest that different types of components might contribute
247 differently to the regulation of gene expression.

248

249

250 **Distinct regulatory components influence gene expression and its evolution differently**

251 To explore the ability of our classification of components to discriminate different regulatory roles,
252 we disentangled the underlying network of regulatory co-dependencies between the different
253 regulatory components and gene expression in our cell-type. For this, we used Sparse Partial
254 Correlation Analysis (SPCA)[24] of the normalized RNA-seq and histone mark enrichments
255 (aggregated by promoter and enhancer state in every type of regulatory component) (Methods). This
256 approach establishes a stringent protocol (Benjamini-Hochberg's correction, $P < 1.8 \times 10^{-22}$ for all
257 selected partial correlations) that selects informative partial correlations[24].

258 To unravel the contribution of each type of component to gene expression, we defined their consensus
259 signal (or eigencomponents) inspired by the notion of eigengenes[25] (Methods). An SPCA based on
260 the eigencomponents shows a consistent global structure of regulatory interactions, with genic
261 promoters and intragenic enhancers directly regulating gene expression coordinately, promoter-
262 interacting enhancers connected with promoters and enhancer-interacting enhancers connected with
263 promoter-interacting enhancers (Fig. 4e and Supplementary Table 12). This regulatory scaffold is
264 consistently observed for the residuals of the histone marks for these eigencomponents
265 (Supplementary Fig. 38 and Supplementary Table 13) when SPCA was performed for all the histone
266 marks together (Supplementary Fig. 39 and Supplementary Table 14) and for each of them separately
267 (Supplementary Figs. 40-44 and Supplementary Table 15). To account for the possibility of
268 incompleteness in some of our architectures, we replicated all the analyses using only genes with full
269 regulatory architectures (i.e., genes associated with regulatory components of every type) obtaining
270 consistent results (Supplementary Figs. 45-52 and Supplementary Table 15).

271 In agreement with the structure of regulatory interactions recovered by our SPCAs, a generalized
272 linear model of gene expression based on H3K27ac, H3K27me3, and H3K36me3 signals at genic
273 promoters and intragenic enhancers and their interactions (15 variables) explains ~67% of gene
274 expression variability (Supplementary Table 16). Remarkably, this is only 6% lower than an
275 exhaustive naive model, including the signal from all histone marks at all types of regulatory
276 components with all possible interactions (1,225 variables) (Supplementary Table 17). These results
277 confirm that the epigenetic activities of genic promoters, intragenic enhancers, and their interactions
278 are likely the most direct determinants of gene expression regulation in our regulatory architectures.
279 However, their co-dependency with the other components suggests that they are dependent, in turn,
280 on the coordination of the whole architecture. These networks reflect that regulatory co-dependencies
281 between components depend on the distance of the elements in the network of chromatin contacts
282 (with genic promoters and intragenic enhancers being in the gene locus, promoter-interacting
283 enhancers interacting directly, and enhancer-interacting enhancers interacting indirectly with it). The

284 robustness of these networks of direct co-dependencies, their ability to explain gene expression, and
285 their correspondence with the spatial disposition of the elements show that these components reflect
286 specific regulatory roles.

287 Previous studies have found that gene expression evolution is associated with changes in the
288 regulatory complexity of a gene (the number of close regulatory elements)[9]. Since we could classify
289 the regulatory elements of a gene into different components (Supplementary Fig. 53), we were able
290 to investigate the association of gene expression changes (Supplementary Figs. 54 and 55) with the
291 evolutionary differences in the complexity of each type of component. We found that the effect of
292 changes in complexity on gene expression levels depends on the epigenetic state gained or lost and
293 the type of regulatory component affected (Supplementary Fig. 55). Evolutionary changes that alter
294 the epigenetic state at genic promoters, specifically the presence of either a strong promoter or poised
295 enhancer, as well as the number of intragenic enhancers with either strong or poised enhancer states,
296 show the most robust associations with gene expression differences (Supplementary Fig. 55). The
297 number of proximal enhancers in any enhancer epigenetic state and strong promoters and strong and
298 poised enhancers in promoter-interacting enhancers also show significant though modest effects
299 (Supplementary Fig. 55). These results highlight that the additive nature of gene regulation depends
300 on regulatory architectures. This dependency can be captured either by the aggregation of histone
301 enrichment signals (as in our SPCAs) or by quantifying the number of regulatory components with
302 specific activities. Moreover, they confirm that our regulatory components represent different
303 regulatory roles with a different contribution to gene expression evolution and which evolutionary
304 relevance should be investigated separately.

305

306 **Poised and weak enhancers in genic promoters and intragenic enhancers appear in brain-**
307 **specific genes with neuronal functions**

308 We next explored to what extent the conservation and species-specificity of the characteristic
309 regulatory states in every component (overrepresented combinations, Supplementary Fig. 56) is
310 important for particular functional processes. For this, we examined their functional annotation and
311 tissue-specificity in their expression (GTEx data[26], Supplementary Table 18). We found significant
312 enrichment for the genes targeted by conserved strong promoter states in genic promoters, conserved
313 strong and weak enhancer states in intragenic enhancers, and conserved poised enhancer states in
314 genic promoters and proximal enhancers (Fisher's exact test: Benjamini-Hochberg's correction, *FDR*
315 < 0.05; Methods, Fig. 5a, Supplementary Fig. 57 and Supplementary Table 19). Remarkably, among

316 the genes associated with species-specific epigenetic states, only those linked to human-specific weak
317 enhancers in intragenic enhancers had significant functional enrichments.

318 These enrichments show the expected association of conserved strong epigenetic states (strong
319 promoter states in genic promoters and strong enhancer ones in intragenic enhancers) with genes
320 involved in relevant cellular processes, such as metabolism, chromatin organization, and regulation
321 of the cell cycle (Fig. 5a, Methods, Supplementary Fig. 57 and Supplementary Tables 20 and 21).
322 Functions specific to LCLs like those involving viral processes are specifically enriched in strong
323 enhancers. Moreover and regardless of whether there is an enrichment, all three strong epigenetic
324 states show similar expression profiles across tissues (Fig. 5b and Supplementary Figs. 58-60), with
325 high expression levels in LCLs and most other tissues and wide expression breadth (Fig. 5c and
326 Supplementary Fig. 61).

327 In contrast, conserved poised enhancer states in genic promoters and proximal enhancers target
328 protein-coding genes enriched in developmental and proliferative functions, echoing their known
329 implication in these processes (Fig. 5a, Supplementary Fig. 57 and Supplementary Tables 22 and 23).
330 Surprisingly, genes with conserved poised enhancer states in their genic promoters are also enriched
331 in neuronal functions and higher expression levels in brain (Fig. 5b-c and Supplementary Figs. 57-
332 60). Genes associated with both types of conserved poised enhancer states show overall minimal
333 expression levels but high tissue-specificity (median tissue specificity index (τ, Tau) > 0.85 in both;
334 Methods and Supplementary Fig. 61).

335 Protein-coding genes targeted by intragenic enhancers with conserved weak enhancer states are
336 enriched in various functional annotations, including neuronal ones, such as cell projection and
337 synapse (Fig. 5a, Supplementary Fig. 57 and Supplementary Table 24). This gene setshows
338 remarkably low expression in LCLs coupled with higher expression in the brain, which is in
339 agreement with the observed functional annotation (Fig. 5b-c). Also, the tissue-specificity of this
340 group is higher than that of conserved strong regulatory activities both in promoters and enhancers
341 (median τ = 0.72, Dwass-Steel-Critchlow-Fligner test: $P < 2.2 \times 10^{-16}$ in the three tests;
342 Supplementary Fig. 61). This apparent brain-specificity is not found in genes associated with other
343 weak enhancer states that have overall higher expression levels and not particular specificity, as
344 would be expected from weak epigenetic states (Supplementary Figs. 60 and 61).

345 Finally, we focused on genes targeted by components with human-specific epigenetic states. These
346 genes are solely enriched in neuron parts and synapse (Fig. 5a and Supplementary Table 25). Similar
347 to genes associated with their analogous conserved group, these genes are typically expressed at low
348 levels with highest expression in tissues unrelated to LCLs, particularly brain, tibial nerve, and

349 testis, while having marginal or no expression in numerous other tissues, including LCLs (Wilcoxon-
350 Nemenyi-McDonald-Thompson test: $P < 1 \times 10^{-4}$; Rank-biserial correlation effect size between brain
351 and LCLs = 0.633; Fig. 5b-c, Supplementary Figs. 58 and 59 and Supplementary Table 26).
352 Remarkably, these genes have higher tissue-specific expression than those with conserved strong but
353 not weak activities in their components (median $\tau = 0.84$, Dwass-Steel-Critchlow-Fligner test: $P <$
354 4.5×10^{-14} when compared to strong activities and $P = 0.06$ compared to genes with weak enhancer
355 states; Supplementary Fig. 61).

356 Intrigued by the high tissue-specificity of the genes with novel human weak enhancers, we sought to
357 identify the tissues driving this tissue-specificity taking its analogous conserved group as reference.
358 Testis and brain are the tissues with the highest number of tissue-specific genes ($\tau_{Tissue} > 0.8$), but
359 most interestingly, whereas the fraction of testis-specific genes is comparable between gene sets
360 (Two-tailed Fisher's exact test: $P = 0.54$, $OR = 1.20$), brain-specific genes are more than 2-fold
361 enriched in genes with human-specific intragenic enhancers (Two-tailed Fisher's exact test: $P = 0.02$,
362 $OR = 2.29$; Supplementary Fig. 62).

363 Altogether these results show that while conserved strong epigenetic states are involved in the
364 regulation of important genes highly expressed in LCLs and other tissues, conserved poised enhancer
365 states and conserved and human-specific weak enhancer states in intragenic enhancers are involved
366 in the regulation of genes marginally expressed in LCLs, but with particular functional roles and
367 tissue-specific expression patterns. These unexpected associations are likely to reflect the importance
368 of particular epigenetic states in certain regulatory components to regulate specific processes.

369

370 **Genes with novel human-specific intragenic weak enhancers are targeted by positive selection**

371 The unanticipated association of the genes targeted by human-specific weak enhancer states in
372 intragenic enhancers with neuronal functions prompted us to study the relationship these genes might
373 have with positive selection. In fact, among the genes associated with intragenic enhancers with novel
374 human-specific weak activities, we found several genes previously proposed as candidates for
375 positive selection in humans[27–30]. Some of these genes are *FOXP2*, *PALMD*, and *ROBO1*, which have
376 known brain-related functions[31–34] or *ADAM18*[35], *CFTR*[36,37], and *TBX15*[38].

377 To assess whether genes with human-specific enhancer states have been targeted by recent human
378 adaptation, we investigated their co-occurrence in genes associated with signals of positive
379 selection[27–30] (Methods and Supplementary Table 27). We found that more than one third (38%) of
380 the genes with novel weak intragenic enhancers are associated with genes targeted by positive

381 selection (Fisher's exact test: P = 6.52 x 10^{-18}, OR = 5.69). The results of this analysis (Fig. 6a)
382 indicates that this enrichment is reflected in a significant association of genes targeted by intragenic
383 enhancers (but not in any other component type), genes targeted by intragenic enhancers with weak
384 enhancer states (but not strong or poised enhancer states) and genes targeted by intragenic enhancers
385 with human-specific weak enhancer states (but not in fully conserved or the remaining weak enhancer
386 states). No enrichment in signals of positive selection is observed for genes with genic promoters
387 showing conserved poised enhancer states, even though they are also involved in brain-specific and
388 neuronal functions.

389 Finally, we explored whether these recently evolved human-specific intragenic enhancers are
390 associated with human-specific mutations. For this, we collected a set of over 2.8 million single
391 nucleotide changes fixed in humans (hSNCs) that differ from fixed variants in the genomes of the
392 remaining non-human primates (Methods and Supplementary Table 27). We observed that the hSNCs
393 density is higher in human-specific intragenic enhancers (Mann-Whitney U test: P = 0.01; Methods
394 and Supplementary Fig. 62). More than one-third of the genes with novel human-specific intragenic
395 enhancers with weak enhancers states and with hSNCs also have signals of positive selection, a
396 proportion very similar to the expected 38% (see above). This result suggests that although human-
397 specific mutations and positive selection signals are both associated with the presence of intragenic
398 enhancers with human-specific weak activities, they are not mutually conditioned. As such, it implies
399 that none of these signals is necessary (nor sufficient) to explain the appearance of intragenic
400 enhancers with human-specific weak activities.

401 Among the 11 genes with both signals of positive selection and hSNCs (Fig. 6b), there are several
402 interesting candidates for adaptive evolution of different traits. Many of these genes are associated
403 with neuronal functions (*ROBO1, CLVS1, SEMA5A, KCNH7, SDK1*, and *ADGRL2*), but also with
404 pigmentation (*LRMDA*) or actin organization in cardiomyocytes (*FHOD3*). Other interesting genes
405 that include human-specific weak intragenic enhancers are only associated with signals of human
406 selection (*FOXP2*, *TNIK*, *ASTN2*, *NPAS3*, or *NTM*) or hSNCs in these enhancers (*PALMD*, *VPS13C*,
407 *IGSF21*, or *CADM2*). Interestingly, we found only one antisense RNA gene, *MEF2C-AS1* showing
408 both signals of positive selection and a human-specific enhancer with hSNCs (Supplementary Fig.
409 63). This gene has been associated with ADHD[39], and its target gene *MEF2C*, is a very well known
410 target of genetic alterations (many of them also affecting *MEF2C-AS1*) associated with severe
411 intellectual disability[40], cerebral malformation[40], or depression[40,41].

412 Remarkably, three human-specific intragenic enhancers accumulate more hSNCs than expected
413 (Randomization test: 10,000 simulations, Bonferroni correction, $P < 0.02$ in all cases; Methods and
414 Supplementary Figs. 63 and 64), a number of enhancers which is also significantly higher than

415 expected (Randomization test: 10,000 simulations, P = 8 x 10^{-4}; Supplementary Fig. 65). Two of
416 these genes are protein-coding genes with known functions in brain cell types and with signals of
417 positive selection. *CLVS1* is a protein-coding gene with brain-specific expression (τ_{Brain} = 0.964)
418 required for the normal morphology of endosomes and lysosomes in neurons[42]. *ROBO1* is a broadly
419 expressed integral membrane protein that participates in axon guidance and neuronal migration (τ =
420 0.388)[43,44] that has also been associated with human speech and language acquisition since the split
421 from chimpanzees[32]. The third enhancer is included in *AC005906.2*, a long intergenic non-protein-
422 coding gene specifically expressed in brain (τ_{Brain} = 1). Interestingly, this gene overlaps with *KCNA1*,
423 a voltage-gated potassium channel with the same brain-specific expression pattern (τ_{Brain} = 0.995) and
424 for which mutations have been associated with neurological malfunctions[45].

425 Our results show that the most common regulatory innovation detected in human LCLs, the presence
426 of human-specific weak enhancer activities in intragenic enhancers, targets neuron-related brain-
427 specific genes that are significantly associated with signals of positive selection and an excess of
428 hSNCs in these components. These DNA changes were especially concentrated in three of them. Two
429 of the genes in which these elements are harbored, *CLVS1* and *ROBO1*, exemplify the confluence of
430 signals of positive selection and excess of hSNCs in human-specific regulatory regions targeting
431 protein-coding genes important for normal neuronal structure, migration, and axon guidance in the
432 human brains.

433

434 **Discussion**

435 The evolution of human and non-human primates is an area of major interest, but ethical, legal, and
436 practical constraints often limit access to direct biological material. In this study, we have generated
437 a unique, comprehensive, and unified dataset of epigenomic landscapes in LCLs for human and four
438 non-human primate species. Despite the artificial nature of our cellular model[46–48], previous studies
439 have shown the value of LCLs as an experimentally convenient model of somatic cells that accurately
440 resembles the phenotype of its cell type of origin[49] and which can be robustly used for comparative
441 studies in humans and primates[12,50–52]. Moreover, its clonality ensures a cell type-specific
442 experimental system reducing the confounding factors associated with cell population diversity in
443 bulk tissue samples.

444 Using this cell model, we reproduced previous observations on the dynamics of the evolution of
445 regulatory elements reported in more distant species using liver samples[7,9,18] which we show can be
446 extrapolated to closely related species (at least for great apes and macaques). Moreover, we have
447 expanded these observations to explain how these dynamics result from the different evolutionary

448 constraints associated with their epigenetic activities. Therefore, we show that considering weak and
449 poised activities is of major relevance to fully understand the evolution of regulatory regions.

450 We also observed that different epigenetic activities have characteristic evolutionary patterns with
451 higher conservation for strong promoter and strong and poised enhancer states. The correlations
452 between epigenetic and sequence conservations are also different for each epigenetic state with higher
453 correlations for strong and poised promoter and enhancer states. These differences are likely due to
454 their different influence on gene expression. Therefore, previously reported higher conservation of
455 promoters probably reflects the often bigger influence of these elements in gene expression. This
456 hypothesis is also confirmed by the lower conservation of promoter states observed in the regulatory
457 architectures of the non-coding genes where strong promoter states are scarce.

458 Here, we have introduced a classification of regulatory elements as components of gene regulatory
459 architectures into genic promoters and intragenic, proximal, promoter-interacting, and enhancer-
460 interacting enhancers. The network of regulatory co-dependencies of these types of components
461 reveals that the epigenetic activities of each type of regulatory component influence gene expression
462 levels differently. In brief, coordinated epigenetic activities in genic promoters and intragenic
463 enhancers form the core of these architectures and explain gene expression levels. Regulatory
464 activities in promoter-interacting enhancers are also coordinated with promoter components, and
465 activities in enhancer-interacting enhancers are associated with promoter-interacting enhancers.
466 These results show that the influence of regulatory components on gene expression reflects the
467 structure of the regulatory architecture.

468 The importance of this structure in gene expression evolution is reflected in the different association
469 of gene expression changes with the regulatory complexity of each activity in the distinct components.
470 The addition or removal of strong promoter activities in promoter components or strong and poised
471 enhancer activities in intragenic enhancers consistently co-occurs with gene expression changes
472 between primate species. The remaining components show fewer changes linked to expression
473 differences, but they can still be instrumental for gene expression evolution, probably through their
474 influence on promoters and intragenic enhancers. Our conceptual framework provides a starting point
475 for future in-depth investigations on the inter-dependence of different regulatory regions and
476 mechanisms in the evolution of gene regulation. In this sense, we stress the importance of considering
477 promoter and enhancer activity states in the different types of gene components to achieve a more
478 detailed description of the regulatory processes.

479 Despite the larger influence of strong activities on gene regulation, our results in LCLs suggest that
480 major insights can arise from the analysis of the elements with a repressive or negligible regulatory

role in our cell model. Genic promoters and proximal enhancers with poised enhancer activities and intragenic enhancers with weak enhancer activities carry information about the degree of regulatory innovation in unrelated cell types. Conserved poised activities are targeted by genes associated with cell proliferation and differentiation. In the case of poised enhancer states in genic promoters, these genes are specifically expressed in brain. Moreover, we found that recently evolved weakly active intragenic enhancers in the human lineage are the most common regulatory innovation observed in our LCLs. These human-specific weak enhancers occur in genes showing patterns of brain-specific gene expression, neuronal functions, and signals of positive selection, suggesting that these genes may have contributed to human adaptation in several traits. These functional and evolutionary patterns are different from those in genes targeted by any conserved activity in any other component, including conserved poised enhancers in genic promoters that also target genes with brain-related functions.

We have identified a subset of genes in which regulatory innovation in these intragenic enhancers converges with other signals of positive selection. Among these genes, we highlight two protein-coding genes key in neuronal structure, migration, or axon guidance: *CLVS1* and *ROBO1*, also accumulating an excess of human-specific mutations in the corresponding human-specific enhancers. The confluence of epigenetic and sequence innovations in the human lineage for these genes points to their putative relevance in recent human evolution. Our findings suggest that the appearance of novel intragenic enhancers with tissue-specific and functionally relevant implications in certain genes is often bound to the co-appearance of weaker activity signals that can be detected in other cell types. These echoes that we detect as human-specific weak enhancer activities provide an unexpected window to the study of regulatory evolution in the human lineage. Further research will be needed to clarify the specific role of these elements in different tissues and cell types.

Taken together, our results show that the evolution of gene regulation is deeply influenced by the coordination of epigenetic activities in gene regulatory architectures. Our insights call for incorporating better integrative datasets and refined definitions of regulatory architectures in comparative evolutionary studies to fully understand the interplay between epigenetic regulation and gene expression.

513 **Methods**

514 **Definition of regulatory elements**

515 We used ChromHMM to jointly learn chromatin states across samples and segment the genome of
516 each sample[17]. ChromHMM implements a multivariate Hidden Markov Model aiming to summarize
517 the combinatorial interactions between multiple chromatin datasets. Bam files from the five histone
518 modifications profiled were binarized into 200 bp density maps. Each bin was discretized in two
519 levels, 0 or 1, depending on their enrichment computed by comparing immunoprecipitated (IP) versus
520 background noise (input) signal within each bin and using a Poisson distribution. Binarization was
521 performed using the BinarizeBam function of the ChromHMM software[17]. A common model across
522 species was learned with the LearnModel ChromHMM function for the concatenated genomes of all
523 samples but O1 (orangutan sample 1) due to its anomalous epigenetic profiles (Supplementary Fig.
524 76). Several models were trained with a number of chromatin states ranging from 8 to 20. To evaluate
525 the different n-state models, for every sample, the overlap and neighborhood enrichments of each
526 state in a series of functional annotations were explored. A 16-state model was selected for further
527 analysis based on the resolution provided by the defined chromatin states, which capture the most
528 significant interactions between histone marks and the state enrichments in function-annotated
529 datasets (Supplementary Fig. 2). The genomic coordinates of regulatory elements (RE) were defined
530 for each sample by merging all consecutive 200 bp bins excluding elongating (E1 and E2), repressed
531 heterochromatin (E16) and low signal (E15) chromatin states. Species regulatory elements were
532 defined as the union of sample regulatory elements. For orangutan we did not include regulatory
533 elements specific to O1.

534 **Assignment of a regulatory state to regulatory elements**

535 Regulatory elements were assigned a chromatin-state based annotation. Combining the information
536 gathered through the overlap and neighborhood enrichment analyses in functionally defined regions,
537 we established a hierarchy to designate poised (p), strong (s) and weak (w) promoter and enhancer
538 states. Chromatin states E8, E9 and E11 defined promoter states (P); E8 and E9 were strongly
539 enriched at TSSs, CGI, UMR (unmethylated regions) and open chromatin regions, while E11 was
540 mostly located downstream the TSS; the presence of E14 defined poised promoter states (pP);
541 absence of E14 and presence of E9 or E11 defined strong promoter states (sP); remaining P were
542 classified as weak promoter states (wP). Non-promoter regulatory elements were assigned an
543 enhancer state (E). The presence of E14 defined poised enhancer states (pE); absence of E14 and
544 presence of E3, E4, E5, E6 and E12 defined strong enhancer states (sE): E5 and E6 were strongly

545 enriched LMRs (low methylated regions) whereas E3, E4 and E12 were highly abundant at introns;
546 remaining E were classified as weak enhancer states (wE) (Supplementary Figs. 2 and 66).

547 One of the limitations of chromatin states is that bin assignments are based on the presence or absence
548 of particular epigenetic marks. However, oftentimes, the lines separating different regulatory
549 elements are blurry: e.g. the distinction between promoter and enhancer states generally resides in the
550 H3K4me3/H3K4me1 balance. Hence, some misclassifications are expected due to insufficient
551 precision of the qualitative classification. Considering the quantitative relationship between co-
552 existing histone modifications can help to accurately annotate epigenetic states in regulatory
553 elements. We used linear discriminant analysis (LDA)[53] to refine chromatin-state based annotations.
554 This method is commonly applied to pattern recognition and category prediction. LDA is a technique
555 developed to transform the features into a lower-dimensional space, which maximizes the ratio of
556 between-class variance to the within-class variance, thereby granting maximum class separation. We
557 performed LDA analysis using the lda function in the R package MASS (version 7.3-47)[54]. The
558 predictor variables were the background-noise normalized IP signals from the five different histone
559 modifications profiled and chromatin accessibility signal at species regulatory elements. The
560 categorical variable to be predicted based on the underlying enrichments was the chromatin-state
561 based annotation. The regulatory state at the species level was determined based on the regulatory
562 state in each of the biological replicates. Thus, the regulatory state of a regulatory element with
563 different epigenetic states in the two replicates (ambiguous), could be aP or aE, when both samples
564 of a given species were annotated as either P or E but differ in their activity; P/E, when a regulatory
565 element was classified as P in one biological replicate and E in the other one; and P/Non-RE or
566 E/Non-RE, when the regulatory elements was so only in one replicate (Supplementary Fig. 7 and
567 Supplementary Table 1). To control for interindividual variability, only regulatory elements with the
568 same activity in the two replicates were considered for downstream analyses.

569 **Analysis of evolutionary conservation at orthologous regulatory regions**

570 We studied patterns of evolutionary conservation of promoter and enhancer states using a set of
571 21,753 one-to-one orthologous regions associated with genes in which at least one species showed a
572 promoter or enhancer epigenetic state. We define *recently repurposed promoters* as orthologous
573 regulatory regions in which one species shows a promoter state while the others show an enhancer
574 state or vice versa. *Novel promoter or enhancer states* refer to those orthologous regulatory regions
575 in which a given species showed a promoter or enhancer state while the others showed no evidence
576 of regulatory activity (classified as *non-regulatory*).

577 To study the patterns of evolutionary conservation of regulatory states, we focused on the subset of
578 10,641 one-to-one orthologous regions in which at least one species showed a strong, poised or weak
579 regulatory state (we do not include orthologous regions including elements with ambiguities, ie.
580 different activities between biological replicates). To statistically assess the different evolutionary
581 dynamics observed for the different regulatory states we first ran randomization analysis. We
582 randomized (1,000 randomizations) the regulatory states associated with each species in orthologous
583 regulatory regions. We determined the P-value as the number of randomizations with an average
584 conservation equal to or above the observed conservation for each regulatory state. We further
585 explored the different patterns of conservation combining: (1) Kruskal-Wallis test (kruskal.test R
586 function)[55] to test whether the global distributions of the number of species in which each particular
587 state was conserved were different for the different regulatory states and (2) Dwass-Steel-Critchlow-
588 Fligner test to assess the significance of every pairwise comparison (dscfAllPairsTest function from
589 the R package PMCMRplus version 1.4.4)[56] and (3) Glass rank biserial correlation coefficient for
590 Mann-Whitney U test to compute the effect sizes associated with all statistically significant pairwise
591 comparisons (wilcoxonRG function from the R package rcompanion version 2.3.25)[57].

592 To study the patterns of evolutionary conservation of the sequence underlying orthologous regulatory
593 regions, we assigned each orthologous regulatory region a conservation score. We computed this
594 score based on the phastCons30way sequence conservation track[19]. To control for background
595 sequence conservation levels, we first computed the average and standard deviations
596 phastCons30way in TADs defined in the cell line GM12878[58] (Supplementary Fig. 25). Then, we
597 used these summary statistics to calculate the z-score for each bp in every orthologous regulatory
598 region, using the average and standard deviations values of the TAD in which each orthologous
599 regulatory region was found. We averaged the z-scores within each orthologous regulatory regions
600 in bins of 200 bp that overlap 50 bp with the next bin and assign each orthologous regulatory region
601 the maximum z-score values associated with its bins. We computed the Spearman rho correlation
602 between the z-scores and the number of species in which each orthologous regulatory region was
603 conserved, separately for each regulatory state. To determine the statistical significance of these
604 correlations we used randomization analysis. For each regulatory state we created 1,000 sets
605 randomizing the z-score associated with each orthologous regulatory region and calculated the
606 Spearman correlation in each randomization. We determined the P-value as the number of
607 randomizations with a Spearman rho correlation value equal to or above the observed correlation
608 (Supplementary Figs. 28-30).

609

610 **Classification of regulatory elements in different types of components of gene regulatory**
611 **architectures**

612 We pre-classified each regulatory element into gene regulatory component based on their genomic
613 location with respect to their corresponding species ENSEMBL release 91[59] gene annotations.
614 Regulatory elements found up to 5 Kb upstream to the nearest TSS were classified as genic promoters
615 (gP). Additional regulatory elements located up to 10 Kb to the nearest TSS were classified as
616 proximal enhancers (prE). Regulatory elements that overlapped a gene were classified as intragenic
617 enhancers (gE). Other regulatory elements that could not be linked to a gene based on their genomic
618 proximity were initially classified as distal enhancers (dE).

619 Then, we made use of available interaction data for the cell line GM12878 (HiC[21], HiChIP-
620 H3K27ac[22] and ChIA-PET[23]) to map interactions between regulatory elements. Each interacting pair
621 was mapped independently to hg38 coordinates using the liftOver tool from the UCSCTOOLS/331
622 suite[60], and only interactions for which both pairs could be mapped were kept. Subsequently,
623 interactions were mapped to the non-human primate reference genome assemblies. For inter-species
624 mappings, coordinates were mapped twice, going forward and backward, and only pairs that could
625 be mapped in both directions were kept. Interacting regulatory elements were defined as those that
626 overlapped with each pair of any given interaction. First-order interactions were annotated between
627 promoters and enhancers, allowing the definition of promoter-interacting enhancers (PiE). Second-
628 order interactions were annotated between enhancer components (gE, prE or PiE), allowing the
629 definition of enhancer-interacting enhancers (EiE) (Fig. 4a and Supplementary Fig. 1).

630 Considering both classifications of regulatory elements, according to their epigenetic state and
631 regulatory component, regulatory elements were separated into 30 (6x5) different subcategories. We
632 used a Chi-square test to identify the component-epigenetic state combinations enriched in
633 orthologous regulatory regions with fully conserved and species-specific epigenetic states
634 (Supplementary Fig. 56).

635 **Gene expression levels and regulatory states in gene components**

636 To investigate the influence of the activity state of regulatory elements in each type of component on
637 gene expression levels, we classified 1-to-1 orthologous protein-coding genes, separately for each
638 species, into six mutually excluding categories, one for each regulatory state within each type of
639 component (component-state combinations). Whereas genes can only be associated with one genic
640 promoter and hence, they can only be classified into one category for genic promoters depending on
641 the corresponding epigenetic state of the regulatory element, genes can be associated with more than
642 enhancer component (gE, prE, PiE and EiE). In those cases we classified genes into a given

643 component-state category accordingly to the presence of at least one regulatory element with a given
644 epigenetic state in that component using the following state hierarchy: pE > pP > sE > sP > wE > wP
645 (Supplementary Fig. 36). To statistically assess the influence of each state in each component we
646 used (1) Kruskal-Wallis test (kruskal.test function as implemented in R)[55] to test whether the
647 distributions of the expression levels of genes associated with each component-state combination
648 were different for the different regulatory states, (2) Dwass-Steel-Critchlow-Fligner test to assess the
649 significance of every pairwise comparison (dscfAllPairsTest function from the R package PCMRplus
650 version 1.4.4)[56] and (3) Glass rank biserial correlation coefficient effect size for Mann-Whitney U
651 test to compute the effect sizes associated with all statistically significant pairwise comparisons
652 (wilcoxonRG function from the R package rcompanion version 2.3.25)[57] (Supplementary Fig. 37).

653 **Partial correlation analysis**

654 To disentangle the network of direct co-dependencies between the different components, regulatory
655 states, histone marks and gene expression, we performed a series of partial correlation analyses[24,61].
656 To tackle the diversity of architectures detected for the different genes, we added up the calibrated
657 signal of all the regulatory elements with a given regulatory state (promoter or enhancer) in a given
658 type of component for any gene architecture. This decision was based on the observed relationship
659 between the number of strong elements in a gene architecture and the expression level of its target
660 gene. Separation of histone signals in each type of component between those contributing to a
661 promoter or to an enhancer was intended to reflect the potential differences in their role in gene
662 expression regulation. As a result of this design, our system has 51 variables (RNA-seq signal + 5
663 histone mark signals x 2 regulatory states x 5 components) and 57,370 cases (5,737 genes x 5 species
664 x 2 samples).

665 All partial correlation analyses were performed using an adaptation of a recently published Sparse
666 Partial Correlation Analysis protocol[24] based on the continuous values of the accumulated ChIP-seq
667 signals (instead of their ranks) to take advantage of their pseudo-quantitative nature. This protocol
668 combines the recovery of statistically significant partial correlations with a cross-validation process
669 to filter out those relationships leading to overfitted reciprocal linear LASSO models (significant
670 partial correlations unlikely to be biologically meaningful). In our case, in every analysis, we
671 recovered those partial correlations recovered in at least four of the five species without leading to
672 overfitting when determining the reciprocal explanatory power in the remaining species. This
673 protocol is intended to detect biologically relevant co-dependences out of the set of significant partial
674 correlations and as a result, this approach filters out many significant partial correlations with very
675 low explanatory power. In fact, all the partial correlations recovered in any of the analyses performed
676 showed very low P-values (Benjamini-Hochberg's correction[62], $P < 1.8 \times 10^{-22}$). In our case, given

677 the relatively small amount of data, we focused on recovering those partial correlations that are likely
678 to be relevant in any species. For these analyses, we used a modified version of the R code provided
679 by the authors (http://spcn.molgen.mpg.de/code/sparse_pcor.R/) to perform 5-fold cross-validation
680 analyses separati by species instead of the original 10-fold cross-validation protocol suitable for larger
681 datasets. Network visualizations were performed with Cytospace[63].

682 In a partial correlation model, direct co-dependencies are established between individual variables.
683 However, we know that coordination of the different histone marks within components is important
684 to define the global epigenetic configuration of a component (also captured in our epigenetic states),
685 which itself could be considered the relevant variable for this analysis. To better address this situation
686 in our analysis, we defined a consensus signal for every component following the same approach
687 established by WGCN[25] to define eigengenes as representative variables of clusters of co-expressed
688 genes. In brief, we defined eigencomponents as the variables summarizing the common signals of the
689 different histone marks in a component (actually calculated as the first PCA component of these five
690 variables). So that eigencomponents keep the meaning of the activities, they were defined as
691 codirectional with H3K27ac signals in each component (eigenvectors negatively correlated with
692 H3K27ac signals were multiplied by -1). We performed a Sparse Partial Correlation Analysis of these
693 10 eigencomponents and RNA-seq that recovers very clearly the structure of direct co-dependecies
694 between the epigenetic configuration of the different components and gene expression (Fig. 4e and
695 Supplementary Table 12).

696 In addition, we defined the remaining unexplained signal of every histone mark by its
697 eigencomponent as the residuals of a linear model of the original variables and the corresponding
698 eigencomponent. A Sparse Partial Correlation Analysis of these residuals (Supplementary Fig. 38
699 and Supplementary Table 13) shows that even these residuals reflect the same inter-component
700 structure and highlights that our eigencomponents miss some relevant information for the definition
701 of this regulatory coordination (mainly weaker co-dependencies involving promoter states in
702 intragenic and promoter-interacting enhancers and enhancer states in promoters).

703 To assess to what extent eigencomponents reflect the behavior of the whole network of co-
704 dependencies of the histone marks or of each of the specific histone marks, we also performed SPCAs
705 using the actual ChIP-seq enrichment signals. A global partial correlation analysis considering all 51
706 variables shows a very clear structure of direct co-dependencies with a strong intra-component
707 contribution for the two states of every single component and a clear but more modest exclusive inter-
708 component contribution (Supplementary Fig. 39 and Supplementary Table 14). Analyses to
709 determine the Sparse Partial Correlation Network of each of the histone marks and RNA-seq without
710 considering the possible influence of the remaining histone marks (Supplementary Figs. 40-44 and

711 Supplementary Table 15) retrieve very similar networks pointing to the common backbone of inter-
712 component co-dependences reflected in our SPCA of the eigencomponents.

713 Our dataset of regulatory components shows a quite unbalanced contribution of the components to
714 the architectures, with intragenic enhancers being the most abundant type of component and
715 promoter-interacting and enhancer-interacting enhancers being the least abundant (Supplementary
716 Fig. 33). These differences could be at least partially related to our inability to recover some of the
717 chromatin interaction-mediated regulatory associations. More importantly, this imbalance, if not real,
718 could affect the ability of our partial correlation networks to reflect the contribution of those
719 components less represented in our datasets. To explore this point, we recovered the subset of genes
720 (an average of 1068 genes per sample) with full architectures (those with at least one element in every
721 type of component) and repeated all the Sparse Partial Correlation Analyses explained above with
722 this dataset of genes. In all the cases, we obtained very similar results, recovering fewer relevant
723 partial correlations due to the smaller number of genes, but with no signal of any relevant difference
724 in the global structure of the coordinated network of components and gene expression (Supplementary
725 Figs. 45-52 and Supplementary Tables 12-15).

726 All the components of the connected network can be very influential in gene expression through their
727 direct or indirect connection with gene expression. However, our Sparse Partial Correlation Networks
728 point consistently to the direct co-dependency of RNA-seq with the genic promoter and intragenic
729 enhancer components and the co-dependency between them. To quantify the explanatory power of
730 these dependencies for gene expression, we performed a simple generalized linear model (glm
731 function as implemented in R[55]) for RNA-seq using H3K27ac, H3K27me3 and H3K36me3 signals
732 in genic promoters and intragenic enhancers and the interactions between them. This model was able
733 to explain 67% of the gene expression variance (Supplementary Table 15), a percentage 5% higher
734 than the 62% explained by a naïve model including the signals of all histone marks in all the
735 components but no interaction between them (Supplementary Table 16), supporting that genic
736 promoters and intragenic enhancers contained nearly all the epigenetic information needed to define
737 gene expression levels in our data.

738 **Differential gene expression analyses**

739 We identified genes with differential expression levels across species using the iDEGES/edgeR
740 pipeline in the R package TCC (version 1.12.1)[64,65] at an FDR of 0.1 and testing all species pairwise
741 comparisons. Then, we determined the patterns of differential expression, species and direction of the
742 gene expression change, using a two-step approach. For every gene, the Q-values obtained in species
743 pairwise comparisons were ordered from smallest to largest. Different expression labels were then

assigned to each species according to the ordered Q-values. Once all species had an assigned label, the average normalized expression values between groups were compared to determine the directionality of the change. We separate differentially expressed genes into two categories: genes with species-specific expression changes and gene with non-species-specific expression changes.

To investigate the relationship between changes in gene expression and changes in the regulatory architecture of a gene, for every type of regulatory component we run a Wilcoxon signed-rank test evaluating whether the number of regulatory elements with a given regulatory state in that particular regulatory component was significantly associated with higher expression levels, for strong and weak activities, or lower expression levels, for poised activities. P-values obtained for each regulatory role were corrected for multiple testing using the Benjamini–Hochberg procedure[62].

Over-representation analyses (ORA) of functional annotations

We defined sets of genes associated with fully conserved and species-specific component-epigenetic state combinations and explored their functional enrichments. To ensure the representativeness of the functional enrichments, for the gene lists associated with each type of component, we excluded genes associated with components with different epigenetic states activities (i.e., genes associated with both conserved strong and weak intragenic enhancers) or associated with both conserved and species-specific components levels (i.e, genes associated with both a conserved and a species-specific weak intragenic enhancer) and kept those gene lists with a minimum of 15 genes for enrichment analyses. Of note, orangutan-specific component-epigenetic state combinations were excluded from the analysis because they were defined using only one LCL replicate (see above) and they are likely to be enriched in inter-individual variable activities.

Over-representation of Gene Ontology (GO) terms was performed using the WebGestaltR function from the R package WebGestaltR (version 0.4.3)[66] with minNum = 25 and remaining default options. This function controls the false discovery rate (FDR) by applying Benjamini-Hochberg procedure (default threshold FDR = 0.05)[62,67]. Previous analyses have shown that recent enhancers tend to occur in the same genes that already have highly conserved enhancers[9]. To control for the particular background of each component, we built different background gene sets including the set of human genes associated with at least one-to-one orthologous regulatory regions of each type of component, hence we have specific and different backgrounds for genic promoters, intragenic enhancers and promoter-interacting enhancers. To represent and compare enriched GO terms between component-state combinations, we performed a clustering of all significantly enriched GO terms using REVIGO[68]. We associated each GO term with the proportion of genes from each component-state combination that overlapped that GO term. In the case of GO terms enriched in more than one gene

777 set, we chose the highest proportion of genes. We used this list as input for REVIGO. Given that
778 REVIGO only reports the clustering of approximately 350 GO terms and our input list was larger
779 than that, we used the R package GofuncR (version 1.8.0)[69] to retrieve the parent GO terms of the
780 remaining unassigned GO terms and add them to the corresponding group as defined by REVIGO.
781 REVIGO group names were manually assigned, taking into account the most representative parent
782 term (Supplementary Table 19).

783 **Analysis of tissue-specific gene expression patterns**

784 We defined sets of human genes associated with fully conserved component-state combinations, and
785 human genes associated with human-specific gains/losses of regulatory elements. Note that these
786 gene lists are not mutually exclusive since a gene can we associated with different types of conserved
787 or species-specific component-state combinations (e.g., a gene with both a human-specific intragenic
788 enhancer with weak activity and a fully conserved intragenic enhancer with a strong activity). We
789 obtained expression levels (median TPM values) across a collection of different tissues from the latest
790 GTEx release (v8)[26]. We only included tissues with at least 70 samples and grouped tissue subregions
791 into the same tissue category, as stated in Supplementary Table 18. For each component-state
792 combination we followed a two-step approach to remove consistently low-expressed genes across
793 tissues. For that we first assigned a value of 0 to all genes with a median expression level below 0.1
794 TPM and then we excluded from the analyses those genes that had an accumulated expression value
795 in all tissues below 0.1xNumber of tissues (n = 29 tissues). For each component-state combination,
796 differences in median expression across tissues were assessed with the Friedman test using the
797 friedman.test function as implemented in R[55]. We used the Wilcoxon-Nemenyi-McDonald-
798 Thompson test implemented in the pWNMT function of the R package NSM3 (version 1.14)[70] to
799 assess whether expression levels were significantly different for all pairwise tissue combinations.
800 Then, we made use of the rank-biserial correlation to calculate the effect sizes for all statistically
801 significant pairwise tests with the wilcoxonPairedRC function of the R package rcompanion (version
802 2.3.25)[57].

803 We then evaluated the tissue-specificity of the genes associated with the different component-state
804 combinations. For this we calculated the tissue specificity index[71] (τ, tau) for each gene, which is
805 defined as:

806 $$\tau = \sum_{i=1}^{N}(1 - x_i)/N \ - 1 \qquad (1)$$

807 where N is the number of tissues and x_i is the expression value normalised by the maximum
808 expression value. This value ranges from 0, for housekeeping genes, to 1, for tissue-specific genes
809 (values above 0.8 are used to identify tissue-specific genes)[72]. Tissue-specificity indices were

810 calculated for all genes included in the latest GTEx release[26]. Gene expression levels (median TMP)
811 of grouped tissue categories (Supplementary Table 18) were normalised within and across tissues
812 before calculating τ as implemented in the R package tispec (version 0.99.0)[73]. The calcTau function
813 from this package provides a tau value for each gene and also a tau expression fraction for each tissue
814 (which also ranges from 0 to 1) that indicates the specificity of a given gene for that tissue.

815 After calculating τ values, we compared their distributions between gene datasets with the Kruskall-
816 Wallis test and assessed the significance of every pairwise comparison with the Dwass-Steel-
817 Critchlow-Fligner test (dscfAllPairsTest function from the R package PMCMRplus version 1.4.4)[56].
818 Glass rank biserial correlation coefficient was used to compute the effect sizes associated with all
819 statistically significant pairwise comparisons using the wilcoxonRG function from the R package
820 rcompanion version 2.3.25[57] ($P < 0.05$).

821 **Association of genes containing intragenic enhancers with signals of positive selection in**
822 **humans**

823 We built a database of human genomic regions with previously detected signals of positive selection
824 in humans[27–29] and selective sweeps in modern compared to archaic humans[30]. BEDtools[74] was used
825 to assign these regions to both protein-coding and non-coding genes following similar criteria to those
826 used for building the gene regulatory architectures (Methods' section *Classification of regulatory*
827 *elements in different types of components of gene regulatory architectures*). We assigned these
828 regions to a protein-coding gene if they were located within the gene or up to 5 Kb upstream of its
829 TSS. Then, we made use of available interaction data for the cell line GM12878 (HiC[21], HiChIP-
830 H3K27ac[22] and ChIA-PET[23]) to assign positively selected regions to their interacting protein-coding
831 genes. We defined the 2,004 genes associated with at least one positively selected region as the set of
832 genes with signals of positive selection in the human lineage. We computed the overlaps between this
833 gene list and the lists of genes associated with the different component-state combinations. We used
834 one or two-tailed Fisher's exact test to assess the enrichment significance.

835 **Analyses of the density of human-fixed single nucleotide changes (hSNCs) in intragenic**
836 **enhancers with weak enhancer states**

837 In order to study the distribution of human-fixed changes in a specific type of regulatory element, we
838 first generated a dataset with human-specific changes. We used sequencing data from a diversity
839 panel of 27 orangutans, 42 gorillas, 11 bonobos and 61 chimpanzees[75–77], as well as 19 modern
840 humans from the 1000 genomes project[78], all mapped to the human reference assembly hg19. We
841 applied a basic filtering for each site in each individual (sequencing coverage >3 and <100), and kept
842 sites where at least half of the individuals in a given species had sufficient data. Furthermore, at least

843 90% of the kept individuals at a given site in a given species had to share the same allele, otherwise
844 the site was labeled as polymorphic in the population. Indels and triallelic sites were removed, and
845 only biallelic sites were kept. We used data from a macaque diversity panel[79], applying the same
846 filters described above. The allele at monomorphic sites was added using bedtools getfasta[74] from the
847 macaque reference genome rheMac8. Since this panel uses the macaque reference genome, we
848 performed a liftover to hg19 using the R package rtracklayer[80] and merged the data with the great ape
849 diversity panel.

850 Lineage-specific changes were retrieved as polymorphisms with sufficient information. Hence,
851 human-specific changes (hSNCs) were defined as positions where each species carry only or mostly
852 one allele within their respective population, the majority of individuals in each population have a
853 genotype call at sufficient coverage, and the human allele differs from the allele in the other
854 populations.

855 BEDtools[74] was used to annotate those hSNCs in conserved or human-specific weak intragenic
856 enhancers and the density of changes was calculated as the number of hSNCs present in each enhancer
857 divided by the length of the enhancer.

858 To determine which human-specific intragenic weak enhancers were enriched in human-specific
859 changes, we compared their density to what would be expected at random. For that, we first
860 established the number of hSNCs that fall in human intragenic enhancers with weak enhancer states
861 associated with 1-to-1 orthologous regulatory regions (our universe of enhancers). In each simulation,
862 this number of mutations was randomly placed in this universe and we computed the density for each
863 of the human-specific weak intragenic enhancers (10,000 simulations). With this approach, we
864 corrected for the differences in the length of the enhancers. The P-value for each enhancer was
865 computed as the number of simulations with a density equal to or above the observed density for that
866 particular enhancer. All P-values were corrected by multiple testing using the Bonferroni method
867 with the number of tests equal to the number of human-specific weak intragenic enhancers.

868 We then assessed whether the number of enhancers that were statistically enriched in hSNCs (or
869 number of *hits*) was greater than what would be expected at random. In order to do that, for each
870 enhancer we defined its mutation density critical value adjusting by multiple testing and using the
871 simulated values. For example, in a hypothetical case of 100 enhancers and 10,000 simulations, for
872 each enhancer we would order its simulated density of hSNCs from smallest to largest and take the
873 5th value as the critical one (given that our chosen alpha equals 5%, but it has to be corrected by 100
874 tests; therefore it becomes 0.05%). Once we established a critical value for each human-specific
875 intragenic weak enhancer, we determined, for each simulation, how many enhancers had a density

equal to or above their corresponding critical value. Finally, we computed the P-value comparing the number of artificial *hits* in each simulation with the number of observed hits.

Acknowledgments: R.G.-P. was supported by a fellowship from MICINN (FPU13/01823). P.E.-C. was supported by a Formació de Personal Investigador fellowship from Generalitat de Catalunya (FI_B00122). M.K. was supported by a Deutsche Forschungsgemeinschaft (DFG) fellowship (KU 3467/1-1) and the Postdoctoral Junior Leader Fellowship Programme from "la Caixa" Banking Foundation (LCF/BQ/PR19/11700002). D.J. was supported by a Juan de la Cierva fellowship (FJCI2016-29558) from MICINN. T.M-B. is supported by funding from the European Research Council (ERC) under the European Union's Horizon 2020 research and innovation programme (grant agreement No. 864203), BFU2017-86471-P (MINECO/FEDER, UE), "Unidad de Excelencia María de Maeztu", funded by the AEI (CEX2018-000792-M), Howard Hughes International Early Career, Obra Social "La Caixa" and Secretaria d'Universitats i Recerca and CERCA Programme del Departament d'Economia i Coneixement de la Generalitat de Catalunya (GRC 2017 SGR 880). G.M., V.D.C. and L.D.C. were supported by grants from the Spanish of Economy, Industry and Competitiveness (MEIC) (BFU2016-75008-P) and G.M. was also supported by the "Convocatoria de Ayudas Fundación BBVA a Investigadores, Innovadores y Creadores Culturales". J.L.G.-S. was supported by the Spanish government (grants BFU2016-74961-P), an institutional grant Unidad de Excelencia María de Maeztu (MDM-2016-0687) and the European Research Council (ERC) under the European Union's Horizon 2020 research and innovation programme (grant agreement No 740041). A.N. was supported by Fondo Europeo de Desarrollo Regional (FEDER) with project grants BFU2016-77961-P and PGC2018- 101927-B-I00 and by the Spanish National Institute of Bioinformatics (PT17/0009/0020). Figs. 1a, 2a, 4a and 6b fully or partially created with BioRender.com.

Author contributions: T.M.-B. and J.L.G.-S. conceived the study; D.J. designed and supervised the analyses; L.D.C. supervised the work of G.M. and V.D.C.; A.B. procured non-human great ape cell lines; A.N. provided helpful insights; R.G.-P., G.M. and V.D.C. performed the experimental work; R.G.-P., P.E.-C., D.J., I.L., M.R. and M.K analyzed the data; D.J., R.G.-P., and P.E.-C. wrote the manuscript with input from all co-authors.

908 **Figures**:

909 **Figure. 1 Overview of the study design and data generated. a,** One human and eight non-human
910 primate lymphoblastoid cell lines (LCLs) were cultured to perform a variety of high-throughput
911 techniques including whole genome sequencing (WGS), whole genome bisulfite sequencing
912 (WGBS), chromatin-accessibility sequencing (ATAC-seq), chromatin immunoprecipitation
913 sequencing (ChIP-seq) targeting five different histone modifications (H3K27me3, H3K4me1,
914 H3K27ac, H3K4me3 and H3K36me3) and transcriptome sequencing (RNA-seq). We integrated
915 previously published datasets from an extensively profiled human LCL (GM12878) to balance the
916 number of human samples (Supplementary Methods). **b,** Number of sequencing reads generated per
917 sample and experiment. Striped lines indicate data retrieved from previously published
918 experiments[81,82].

919 **Figure 2. Epigenetic and regulatory characterization of regulatory elements annotated in**
920 **primates. a,** Approach followed to annotate and classify regulatory elements (RE). In short, promoter
921 and enhancer states with three activity levels (strong, poised or weak) were annotated for DNA
922 regions based on a combination of chromatin marks and ATAC-seq signals. Regulatory elements
923 (RE) were then linked to genes based on 1D gene proximity and 3D published chromatin maps for
924 LCLs. RE not associated with any gene are referred to as orphan RE. Extended representation in
925 Supplementary Fig. 1. **b,** Number of regulatory elements with promoter and enhancer epigenetic
926 states in each species. **c,** Number of regulatory elements associated with genes and orphan regulatory
927 elements in each species. Genes are divided in 1-to-1 orthologous protein-coding (1-1 orth PC),
928 protein-coding (PC) and non-protein-coding genes. Dashed lines in **b**, and **c**, indicates the average
929 number of RE with promoter and enhancer states annotated across species.

930 **Figure 3. Different regulatory activities have different patterns of epigenetic and sequence**
931 **conservation. a,** Barplots show the average number of orthologous regulatory regions across species
932 with the corresponding color-coded epigenetic state conserved in 1, 2, 3, 4 or 5 species. **b,** Distribution
933 of the sequence conservation scores (calculated as z-scores of the distribution of phastCons30way[19]
934 values for non-coding regions in the same Topologically Associated Domain[58]; Methods) of human
935 orthologous regulatory regions with different epigenetic states conserved in 1, 2, 3, 4 or 5 of our
936 primate species.

937 **Figure 4. Epigenetic signals in gene regulatory architectures explain gene expression levels. a,**
938 Classification of regulatory elements according to their regulatory roles in gene architectures. Of note,
939 EiE may interact with any type of enhancer in a regulatory architecture (prE, gE, PiE and EiE). **b,**
940 Average number of orthologous protein-coding genes associated with each type of regulatory

941 element. **c,** Average number of regulatory elements across species associated with 1-to-1 orthologous
942 protein-coding genes classified as gP, gE, prE, PiE and EiE. Error bars show the standard deviation
943 across species and differently shaped dots show the number corresponding to each species. **d,**
944 Proportion of regulatory elements with a given epigenetic state associated with 1-to-1 orthologous
945 protein-coding genes for each type of regulatory component. Dots and error bars show the average
946 proportion and standard deviation across species, respectively. **e,** Sparse Partial Correlation Networks
947 showing the statistical co-dependence of the RNA-seq (Gene expression) and the consensus ChIP-
948 seq signals for the five histone marks in the every component represented by the eigencomponents
949 (minimal partial correlation = -0.41; maximal partial correlation = 0.33; all partial correlations
950 Benjamini-Hochberg's $P < 4.1 \times 10^{-303}$). Edge widths are proportional to absolute partial correlation
951 values within each network. The networks are based on the 5,737 1-to-1 orthologous protein-coding
952 genes associated with at least one regulatory element in all species. Only nodes for values with
953 significant and relevant partial correlations are represented.

954 **Figure 5. Weak and poised enhancer states echo brain-specific regulation. a,** Functional
955 enrichment of conserved and human-specific activities in genic promoters and intragenic enhancers.
956 The size of circles indicates the proportion of genes included in each functional category from the
957 total number of genes contained in the corresponding regulatory group. Number of genes in each
958 category and extended functional annotation in Supplementary Fig. 57. **b,** Heatmap of standardised
959 expression across tissues in state/component regulatory groups with functional enrichments. Number
960 of genes included in each category and representation with groups without functional enrichment in
961 Supplementary Fig. 58. **c,** Median expression levels in testes, LCLS, brain and whole blood of genes
962 groups in b.

963 **Figure 6. Intragenic enhancers with weak activities co-localize with signals of recent human**
964 **selection. a,** Specific enrichment of genes with signals of positive selection in genes that harbor
965 human-specific intragenic enhancers with a weak enhancer state. Epigenetic states for each species
966 are depicted in white, grey or blue boxes. **b,** Top: Schematic representation of a human-specific
967 intragenic weak enhancer with a hSNC (nucleotide change in humans shown in red) contained in a
968 gene with signals of selection. Bottom: Venn diagram illustrating the overlap between the 41 genes
969 containing human-specific weak intragenic enhancers with signals of selection and the 30 genes with
970 these enhancers and with human single nucleotide changes (hSNCs) fixed in humans and distinct
971 from other non-human primates.

972

973

974 **References**

975 1. Britten, R. J. & Davidson, E. H. Gene Regulation for Higher Cells: A Theory. *Science* vol. 165
976 349–357 (1969).

977 2. Britten, R. J. & Davidson, E. H. Repetitive and Non-Repetitive DNA Sequences and a
978 Speculation on the Origins of Evolutionary Novelty. *The Quarterly Review of Biology* vol. 46
979 111–138 (1971).

980 3. Zhu, Y. *et al.* Spatiotemporal transcriptomic divergence across human and macaque brain
981 development. *Science* **362**, (2018).

982 4. Cardoso-Moreira, M. *et al.* Gene expression across mammalian organ development. *Nature* **571**,
983 505–509 (2019).

984 5. Xu, C. *et al.* Human-specific features of spatial gene expression and regulation in eight brain
985 regions. *Genome Research* vol. 28 1097–1110 (2018).

986 6. Brawand, D. *et al.* The evolution of gene expression levels in mammalian organs. *Nature* vol.
987 478 343–348 (2011).

988 7. Villar, D. *et al.* Enhancer evolution across 20 mammalian species. *Cell* **160**, 554–566 (2015).

989 8. Vermunt, M. W. *et al.* Epigenomic annotation of gene regulatory alterations during evolution of
990 the primate brain. *Nat. Neurosci.* **19**, 494–503 (2016).

991 9. Berthelot, C., Villar, D., Horvath, J. E., Odom, D. T. & Flicek, P. Complexity and conservation
992 of regulatory landscapes underlie evolutionary resilience of mammalian gene expression. *Nat*
993 *Ecol Evol* **2**, 152–163 (2018).

994 10. Reilly, S. K. *et al.* Evolutionary genomics. Evolutionary changes in promoter and enhancer
995 activity during human corticogenesis. *Science* **347**, 1155–1159 (2015).

996 11. Prescott, S. L. *et al.* Enhancer divergence and cis-regulatory evolution in the human and chimp
997 neural crest. *Cell* **163**, 68–83 (2015).

998 12. Zhou, X. *et al.* Epigenetic modifications are associated with inter-species gene expression
999 variation in primates. *Genome Biol.* **15**, 547 (2014).

1000 13. Zeng, J. *et al.* Divergent whole-genome methylation maps of human and chimpanzee brains
1001 reveal epigenetic basis of human regulatory evolution. *Am. J. Hum. Genet.* **91**, 455–465 (2012).

1002 14. Hernando-Herraez, I. *et al.* The interplay between DNA methylation and sequence divergence in
1003 recent human evolution. *Nucleic Acids Res.* **43**, 8204–8214 (2015).

1004 15. Hernando-Herraez, I. *et al.* Dynamics of DNA Methylation in Recent Human and Great Ape
1005 Evolution. *PLoS Genetics* vol. 9 e1003763 (2013).

1006 16. Lowdon, R. F., Jang, H. S. & Wang, T. Evolution of Epigenetic Regulation in Vertebrate
1007 Genomes. *Trends in Genetics* vol. 32 269–283 (2016).

1008 17. Ernst, J. & Kellis, M. Chromatin-state discovery and genome annotation with ChromHMM. *Nat.*
1009 *Protoc.* **12**, 2478–2492 (2017).

1010 18. Carelli, F. N., Liechti, A., Halbert, J., Warnefors, M. & Kaessmann, H. Repurposing of promoters
1011 and enhancers during mammalian evolution. *Nat. Commun.* **9**, 4066 (2018).

1012 19. Siepel, A. *et al.* Evolutionarily conserved elements in vertebrate, insect, worm, and yeast
1013 genomes. *Genome Res.* **15**, 1034–1050 (2005).

1014 20. Ong, C.-T. & Corces, V. G. Enhancer function: new insights into the regulation of tissue-specific
1015 gene expression. *Nat. Rev. Genet.* **12**, 283–293 (2011).

1016 21. Rao, S. S. P. *et al.* A 3D Map of the Human Genome at Kilobase Resolution Reveals Principles
1017 of Chromatin Looping. *Cell* vol. 159 1665–1680 (2014).

1018 22. Mumbach, M. R. *et al.* Enhancer connectome in primary human cells identifies target genes of
1019 disease-associated DNA elements. *Nature Genetics* vol. 49 1602–1612 (2017).

1020 23. Tang, Z. *et al.* CTCF-Mediated Human 3D Genome Architecture Reveals Chromatin Topology
1021 for Transcription. *Cell* vol. 163 1611–1627 (2015).

1022 24. Lasserre, J., Chung, H.-R. & Vingron, M. Finding Associations among Histone Modifications
1023 Using Sparse Partial Correlation Networks. *PLoS Comput. Biol.* **9**, e1003168 (2013).

1024 25. Langfelder, P. & Horvath, S. WGCNA: an R package for weighted correlation network analysis.
1025 *BMC Bioinformatics* **9**, 1–13 (2008).

1026 26. Consortium, T. G. & The GTEx Consortium. The GTEx Consortium atlas of genetic regulatory
1027 effects across human tissues. *Science* vol. 369 1318–1330 (2020).

1028 27. Lindblad-Toh, K. *et al.* A high-resolution map of human evolutionary constraint using 29
1029 mammals. *Nature* vol. 478 476–482 (2011).

1030 28. Prabhakar, S., Noonan, J. P., Pääbo, S. & Rubin, E. M. Accelerated evolution of conserved
1031 noncoding sequences in humans. *Science* **314**, 786 (2006).

1032 29. Gittelman, R. M. *et al.* Comprehensive identification and analysis of human accelerated
1033 regulatory DNA. *Genome Research* vol. 25 1245–1255 (2015).

1034 30. Peyrégne, S., Boyle, M. J., Dannemann, M. & Prüfer, K. Detecting ancient positive selection in
1035 humans using extended lineage sorting. *Genome Research* vol. 27 1563–1572 (2017).

1036 31. Enard, W. *et al.* Molecular evolution of FOXP2, a gene involved in speech and language. *Nature*
1037 vol. 418 869–872 (2002).

1038 32. Mozzi, A. *et al.* The evolutionary history of genes involved in spoken and written language:
1039 beyond FOXP2. *Sci. Rep.* **6**, 22157 (2016).

1040 33. Kalebic, N. *et al.* Neocortical Expansion Due to Increased Proliferation of Basal Progenitors Is
1041 Linked to Changes in Their Morphology. *Cell Stem Cell* vol. 24 535–550.e9 (2019).

1042 34. Kuhlwilm, M. & Boeckx, C. A catalog of single nucleotide changes distinguishing modern
1043 humans from archaic hominins. *Scientific Reports* vol. 9 (2019).

1044 35. Finn, S. & Civetta, A. Sexual Selection and the Molecular Evolution of ADAM Proteins. *Journal*
1045 *of Molecular Evolution* vol. 71 231–240 (2010).

1046 36. Riordan, J. R. Identification of the cystic fibrosis gene: Cloning and characterization of
1047 complementary DNA. *Trends in Genetics* vol. 5 363 (1989).

1048 37. Poolman, E. M. & Galvani, A. P. Evaluating candidate agents of selective pressure for cystic
1049 fibrosis. *Journal of The Royal Society Interface* vol. 4 91–98 (2007).

1050 38. Racimo, F. *et al.* Archaic adaptive introgression in TBX15/WARS2. *Molecular Biology and*
1051 *Evolution* msw283 (2016) doi:10.1093/molbev/msw283.

1052 39. Demontis, D. *et al.* Discovery of the first genome-wide significant risk loci for attention
1053 deficit/hyperactivity disorder. *Nat. Genet.* **51**, 63–75 (2019).

1054 40. Meur, N. L. *et al.* MEF2C haploinsufficiency caused by either microdeletion of the 5q14.3 region
1055 or mutation is responsible for severe mental retardation with stereotypic movements, epilepsy
1056 and/or cerebral malformations. *Journal of Medical Genetics* vol. 47 22–29 (2010).

1057 41. Hyde, C. L. *et al.* Identification of 15 genetic loci associated with risk of major depression in
1058 individuals of European descent. *Nature Genetics* vol. 48 1031–1036 (2016).

1059 42. Katoh, Y. *et al.* The clavesin family, neuron-specific lipid- and clathrin-binding Sec14 proteins
1060 regulating lysosomal morphology. *J. Biol. Chem.* **284**, 27646–27654 (2009).

1061 43. Long, H. *et al.* Conserved roles for Slit and Robo proteins in midline commissural axon guidance.
1062 *Neuron* **42**, 213–223 (2004).

1063 44. Andrews, W. *et al.* Robo1 regulates the development of major axon tracts and interneuron
1064 migration in the forebrain. *Development* **133**, 2243–2252 (2006).

1065 45. Yin, X.-M. *et al.* Familial paroxysmal kinesigenic dyskinesia is associated with mutations in the
1066 KCNA1 gene. *Hum. Mol. Genet.* **27**, 757–758 (2018).

1067 46. Carter, K. L., Cahir-McFarland, E. & Kieff, E. Epstein-Barr Virus-Induced Changes in B-
1068 Lymphocyte Gene Expression. *Journal of Virology* vol. 76 10427–10436 (2002).

1069 47. Hansen, K. D. *et al.* Increased methylation variation in epigenetic domains across cancer types.
1070 *Nat. Genet.* **43**, 768–775 (2011).

1071 48. Sugawara, H. *et al.* Comprehensive DNA methylation analysis of human peripheral blood
1072 leukocytes and lymphoblastoid cell lines. *Epigenetics* **6**, 508–515 (2011).

1073 49. Hussain, T. & Mulherkar, R. Lymphoblastoid Cell lines: a Continuous in Vitro Source of Cells
1074 to Study Carcinogen Sensitivity and DNA Repair. *Int J Mol Cell Med* **1**, 75–87 (2012).

1075 50. Khaitovich, P., Enard, W., Lachmann, M. & Pääbo, S. Evolution of primate gene expression.
1076 *Nature Reviews Genetics* vol. 7 693–702 (2006).

1077 51. Pai, A. A., Bell, J. T., Marioni, J. C., Pritchard, J. K. & Gilad, Y. A genome-wide study of DNA
1078 methylation patterns and gene expression levels in multiple human and chimpanzee tissues. *PLoS*
1079 *Genet.* **7**, e1001316 (2011).

1080 52. Shibata, Y. *et al.* Extensive evolutionary changes in regulatory element activity during human
1081 origins are associated with altered gene expression and positive selection. *PLoS Genet.* **8**,
1082 e1002789 (2012).

1083 53. Tharwat, A., Gaber, T., Ibrahim, A. & Hassanien, A. E. Linear discriminant analysis: A detailed
1084 tutorial. *AI Communications* vol. 30 169–190 (2017).

1085 54. Venables, W. N. & Ripley, B. D. *Modern Applied Statistics with S*. (Springer, New York, 2002).

1086 55. R Core Team. R: A language and environment for statistical computing.

1087 56. Pohlert, T. PMCMRplus: Calculate Pairwise Multiple Comparisons of Mean Rank Sums
1088 Extended. (2020).

1089 57. Mangiafico, S. rcompanion: Functions to Support Extension Education Program Evaluation.
1090 (2020).

1091 58. Wang, Y. *et al.* The 3D Genome Browser: a web-based browser for visualizing 3D genome
1092 organization and long-range chromatin interactions. *Genome Biology* vol. 19 (2018).

1093 59. Aken, B. L. *et al.* Ensembl 2017. *Nucleic Acids Res.* **45**, D635–D642 (2017).

1094 60. Kuhn, R. M., Haussler, D. & Kent, W. J. The UCSC genome browser and associated tools.
1095 *Briefings in Bioinformatics* vol. 14 144–161 (2013).

1096 61. Juan, D. *et al.* Epigenomic Co-localization and Co-evolution Reveal a Key Role for 5hmC as a
1097 Communication Hub in the Chromatin Network of ESCs. *Cell Rep.* **14**, 1246–1257 (2016).

1098 62. Benjamini, Y., Drai, D., Elmer, G., Kafkafi, N. & Golani, I. Controlling the false discovery rate
1099 in behavior genetics research. *Behavioural brain research* vol. 125 279–284 (2001).

1100 63. Shannon, P. *et al.* Cytoscape: a software environment for integrated models of biomolecular
1101 interaction networks. *Genome Res.* **13**, 2498–2504 (2003).

1102 64. Bolstad, B. M., Irizarry, R. A., Astrand, M. & Speed, T. P. A comparison of normalization
1103 methods for high density oligonucleotide array data based on variance and bias. *Bioinformatics*
1104 vol. 19 185–193 (2003).

1105 65. Sun, J., Nishiyama, T., Shimizu, K. & Kadota, K. TCC: an R package for comparing tag count
1106 data with robust normalization strategies. *BMC Bioinformatics* vol. 14 219 (2013).

1107 66. Wang, J. & Liao, Y. *WebGestaltR: Gene Set Analysis Toolkit WebGestaltR*. (2020).

1108 67. Liao, Y., Wang, J., Jaehnig, E. J., Shi, Z. & Zhang, B. WebGestalt 2019: gene set analysis toolkit
1109 with revamped UIs and APIs. *Nucleic Acids Res.* **47**, W199–W205 (2019).

1110 68. Supek, F., Bošnjak, M., Škunca, N. & Šmuc, T. REVIGO Summarizes and Visualizes Long Lists
1111 of Gene Ontology Terms. *PLoS One* **6**, e21800 (2011).

1112 69. Grote, S. GOfuncR: Gene ontology enrichment using FUNC. (2020).

1113 70. Grant Schneider, E. C. A. R. B. NSM3: Functions and Datasets to Accompany. (2020).

1114 71. Yanai, I. *et al.* Genome-wide midrange transcription profiles reveal expression level

1115 relationships in human tissue specification. *Bioinformatics* **21**, 650–659 (2005).

1116 72. Kryuchkova, N. & Robinson-Rechavi, M. A benchmark of gene expression tissue-specificity
1117 metrics. doi:10.1101/027755.

1118 73. Condon, K. tispec: Calculates tissue specificity from RNA-seq data. (2020).

1119 74. Quinlan, A. R. & Hall, I. M. BEDTools: a flexible suite of utilities for comparing genomic
1120 features. *Bioinformatics* **26**, 841–842 (2010).

1121 75. Prado-Martinez, J. *et al.* Great ape genetic diversity and population history. *Nature* **499**, 471–
1122 475 (2013).

1123 76. de Manuel, M. *et al.* Chimpanzee genomic diversity reveals ancient admixture with bonobos.
1124 *Science* **354**, 477–481 (2016).

1125 77. Nater, A. *et al.* Morphometric, Behavioral, and Genomic Evidence for a New Orangutan Species.
1126 *Curr. Biol.* **27**, 3576–3577 (2017).

1127 78. Consortium, T. 1000 G. P. & The 1000 Genomes Project Consortium. A global reference for
1128 human genetic variation. *Nature* vol. 526 68–74 (2015).

1129 79. Xue, C. *et al.* The population genomics of rhesus macaques (Macaca mulatta) based on whole-
1130 genome sequences. *Genome Res.* **26**, 1651–1662 (2016).

1131 80. Lawrence, M., Gentleman, R. & Carey, V. rtracklayer: an R package for interfacing with genome
1132 browsers. *Bioinformatics* vol. 25 1841–1842 (2009).

1133 81. Kasowski, M. *et al.* Extensive variation in chromatin states across humans. *Science* **342**, 750–
1134 752 (2013).

1135 82. Buenrostro, J. D., Giresi, P. G., Zaba, L. C., Chang, H. Y. & Greenleaf, W. J. Transposition of
1136 native chromatin for fast and sensitive epigenomic profiling of open chromatin, DNA-binding
1137 proteins and nucleosome position. *Nat. Methods* **10**, 1213–1218 (2013).

1138

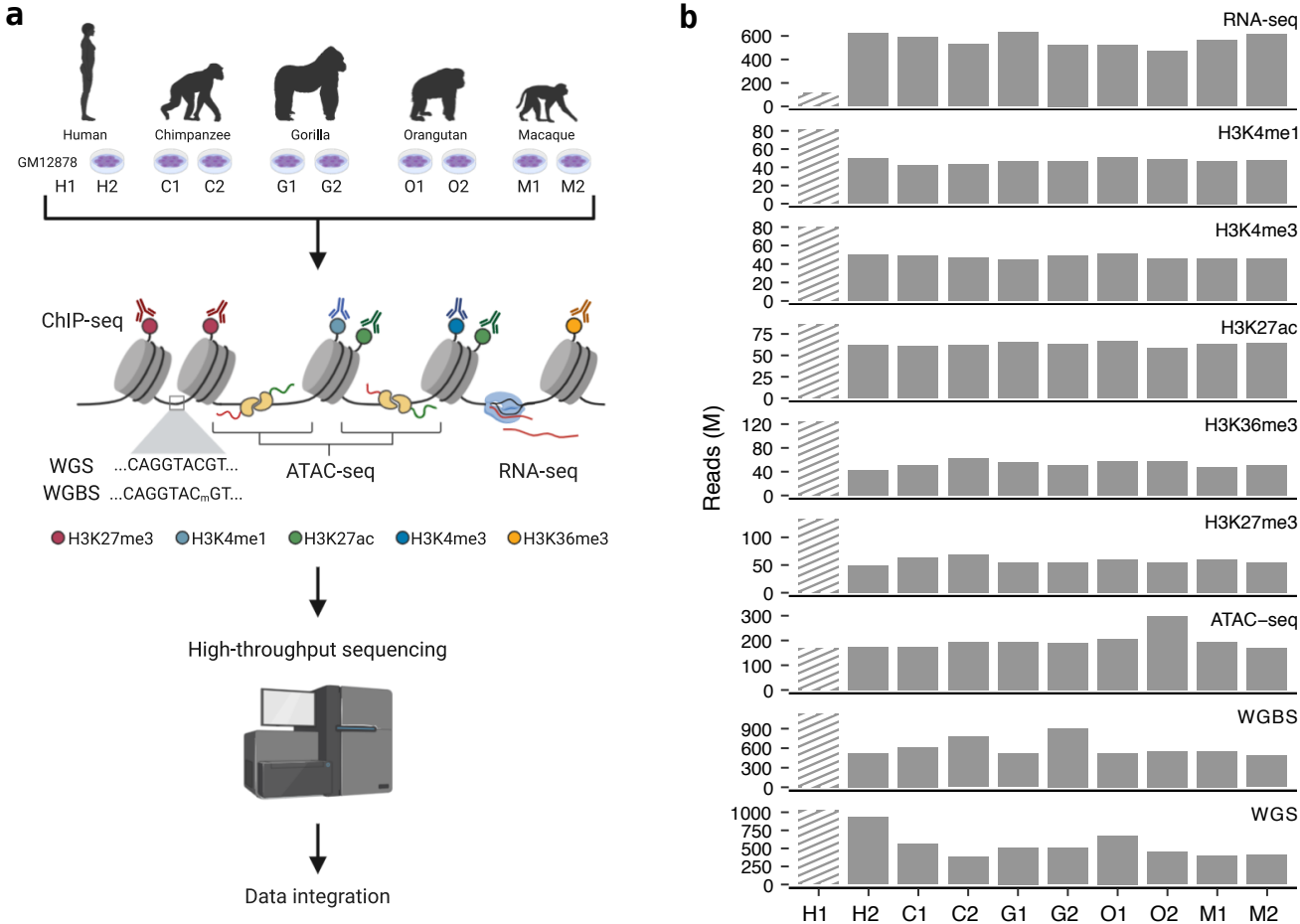
a
Human
Chimpanzee
Gorilla
Orangutan
Macaque
GM12878
H1 H2 C1 C2 G1 G2 O1 O2 M1 M2
ChIP-seq
WGS ...CAGGTACGT...
WGBS ...CAGGTAC$_m$GT...
ATAC-seq
RNA-seq
H3K27me3 H3K4me1 H3K27ac H3K4me3 H3K36me3
High-throughput sequencing
Data integration
b
RNA-seq
H3K4me1
H3K4me3
H3K27ac
H3K36me3
H3K27me3
ATAC–seq
WGBS
WGS
Reads (M)
H1 H2 C1 C2 G1 G2 O1 O2 M1 M2

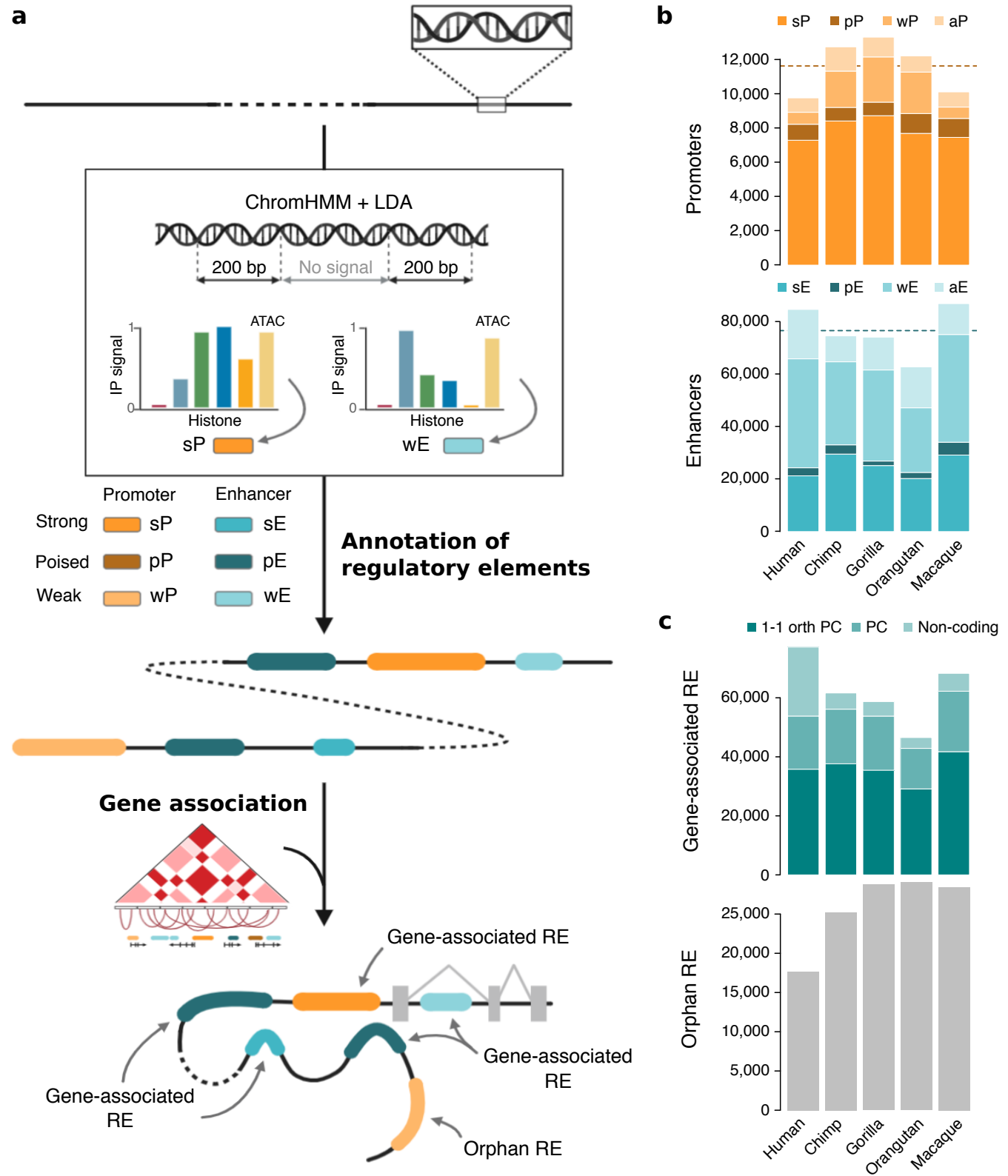
a
ChromHMM + LDA
200 bp
No signal
200 bp
ATAC
IP signal
Histone
sP
ATAC
IP signal
Histone
wE
Promoter
Enhancer
Strong
sP
sE
Poised
pP
pE
Weak
wP
wE
Annotation of regulatory elements
Gene association
Gene-associated RE
Gene-associated RE
Gene-associated RE
Orphan RE
b
sP
pP
wP
aP
Promoters
12,000
10,000
8,000
6,000
4,000
2,000
0
sE
pE
wE
aE
Enhancers
80,000
60,000
40,000
20,000
0
Human
Chimp
Gorilla
Orangutan
Macaque
c
1-1 orth PC
PC
Non-coding
Gene-associated RE
60,000
40,000
20,000
0
Orphan RE
25,000
20,000
15,000
10,000
5,000
0
Human
Chimp
Gorilla
Orangutan
Macaque

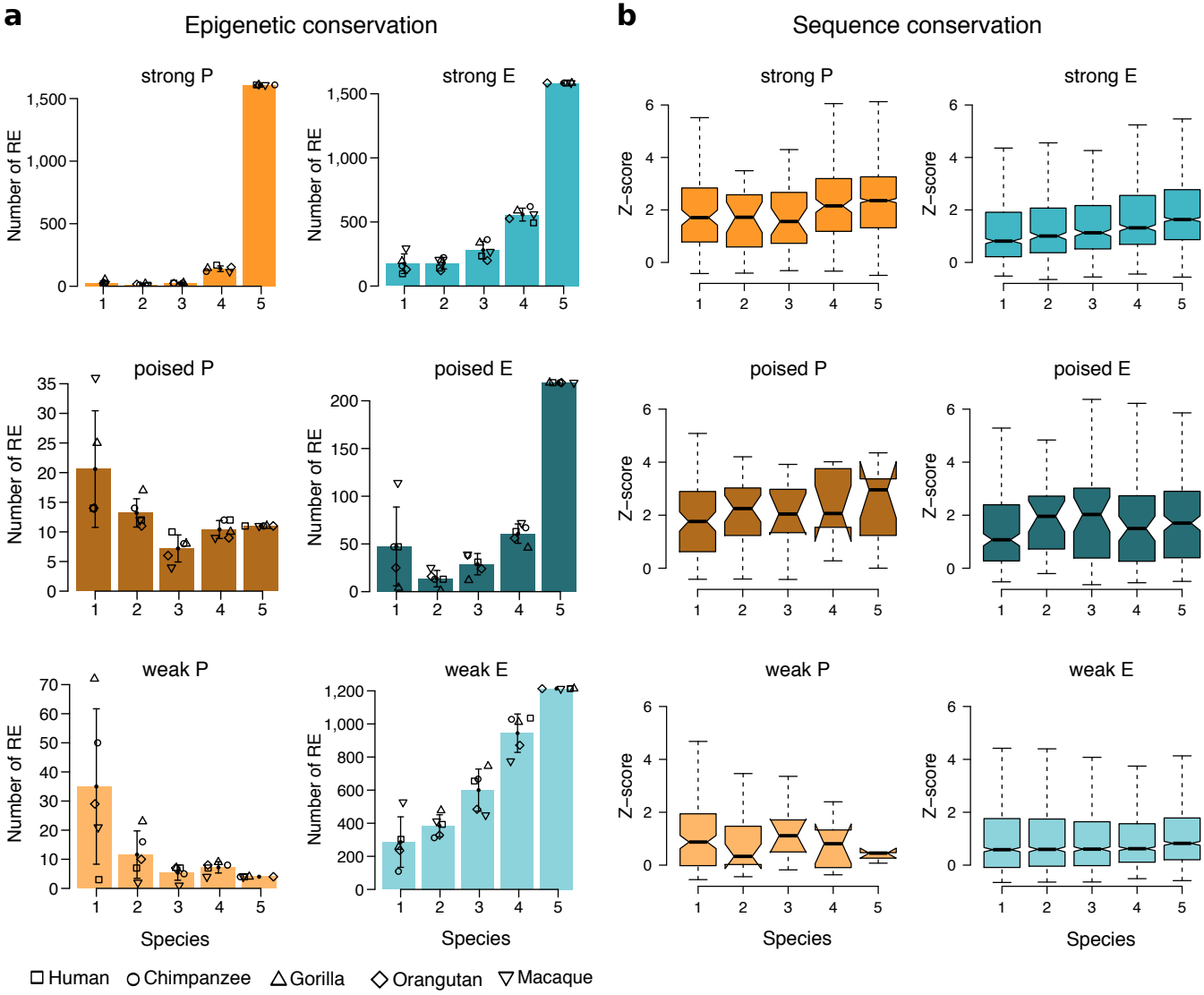
a
Epigenetic conservation
b
Sequence conservation
strong P
strong E
poised P
poised E
weak P
weak E
Number of RE
Z−score
Species
Human
Chimpanzee
Gorilla
Orangutan
Macaque

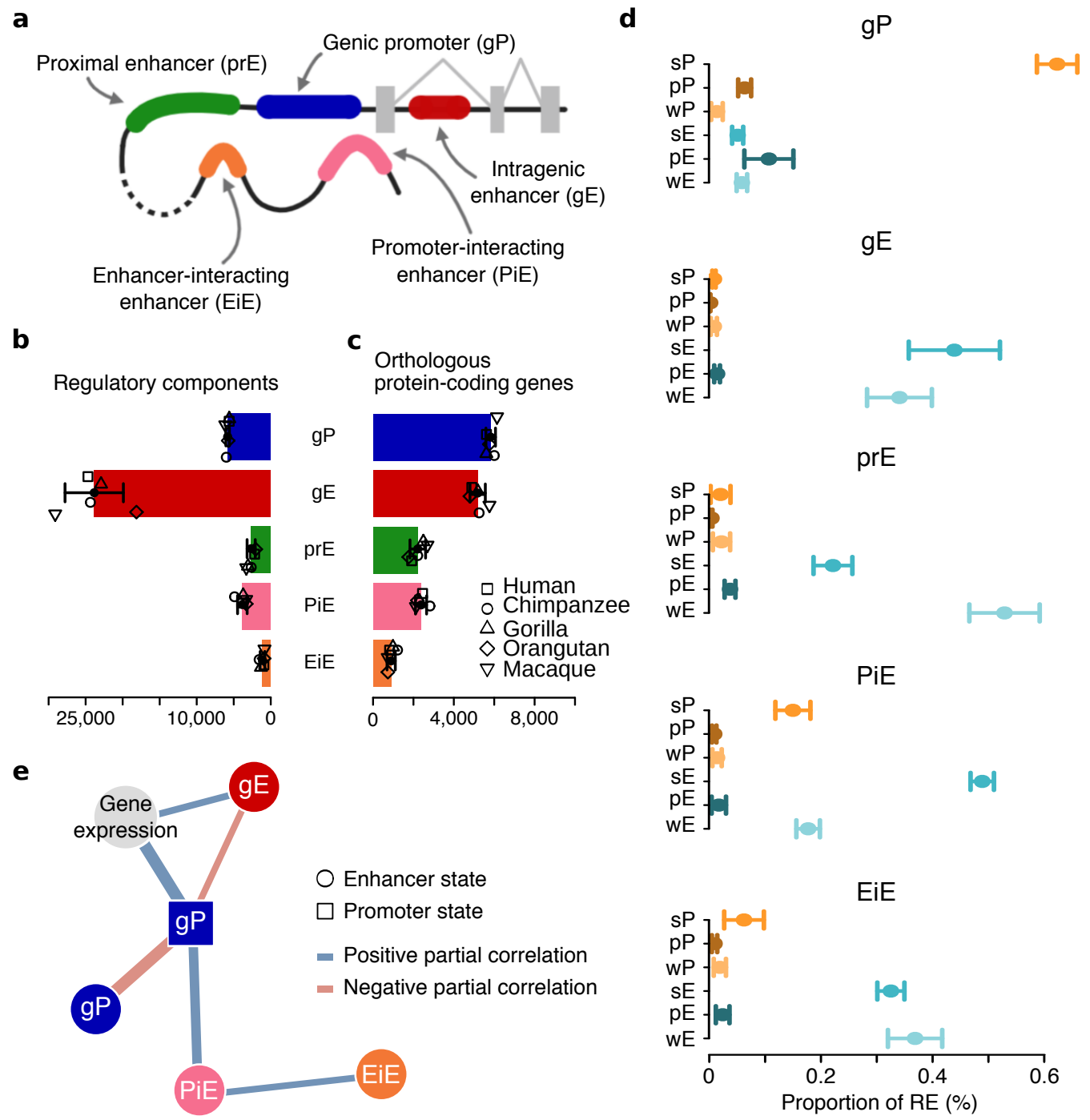
a
Proximal enhancer (prE)
Genic promoter (gP)
Intragenic enhancer (gE)
Promoter-interacting enhancer (PiE)
Enhancer-interacting enhancer (EiE)
b
Regulatory components
gP
gE
prE
PiE
EiE
25,000
10,000
0
c
Orthologous protein-coding genes
0
4,000
8,000
Human
Chimpanzee
Gorilla
Orangutan
Macaque
d
gP
gE
prE
PiE
EiE
sP
pP
wP
sE
pE
wE
0
0.2
0.4
0.6
Proportion of RE (%)
e
Gene expression
gE
gP
gP
PiE
EiE
Enhancer state
Promoter state
Positive partial correlation
Negative partial correlation

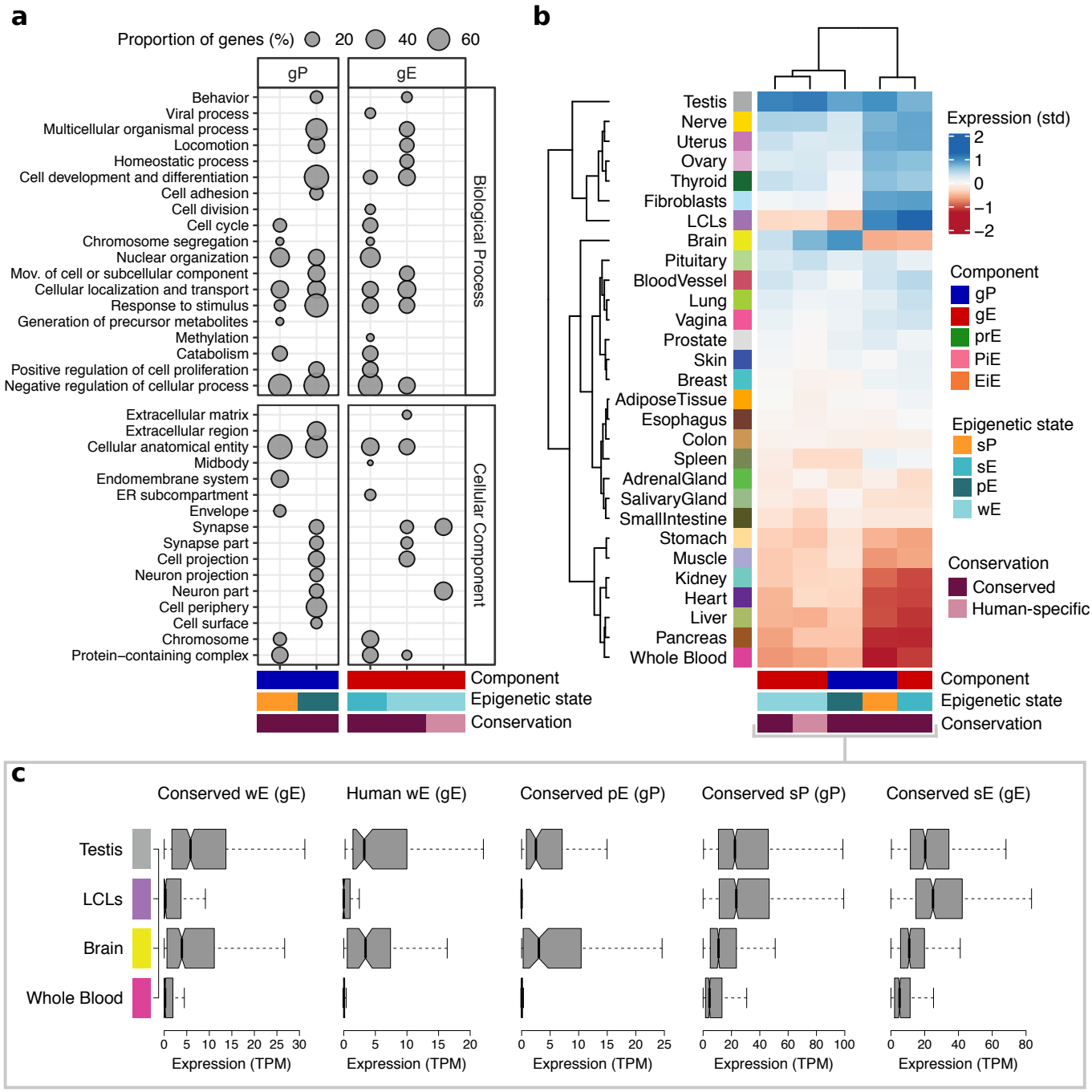
a
Proportion of genes (%)
20
40
60
gP
gE
Behavior
Viral process
Multicellular organismal process
Locomotion
Homeostatic process
Cell development and differentiation
Cell adhesion
Cell division
Cell cycle
Chromosome segregation
Nuclear organization
Mov. of cell or subcellular component
Cellular localization and transport
Response to stimulus
Generation of precursor metabolites
Methylation
Catabolism
Positive regulation of cell proliferation
Negative regulation of cellular process
Biological Process
Extracellular matrix
Extracellular region
Cellular anatomical entity
Midbody
Endomembrane system
ER subcompartment
Envelope
Synapse
Synapse part
Cell projection
Neuron projection
Neuron part
Cell periphery
Cell surface
Chromosome
Protein−containing complex
Cellular Component
Component
Epigenetic state
Conservation
b
Testis
Nerve
Uterus
Ovary
Thyroid
Fibroblasts
LCLs
Brain
Pituitary
BloodVessel
Lung
Vagina
Prostate
Skin
Breast
AdiposeTissue
Esophagus
Colon
Spleen
AdrenalGland
SalivaryGland
SmallIntestine
Stomach
Muscle
Kidney
Heart
Liver
Pancreas
Whole Blood
Expression (std)
2
1
0
−1
−2
Component
gP
gE
prE
PiE
EiE
Epigenetic state
sP
sE
pE
wE
Conservation
Conserved
Human-specific
Component
Epigenetic state
Conservation
c
Conserved wE (gE)
Human wE (gE)
Conserved pE (gP)
Conserved sP (gP)
Conserved sE (gE)
Testis
LCLs
Brain
Whole Blood
0 5 10 15 20 25 30
0 5 10 15 20
0 5 10 15 20 25
0 20 40 60 80 100
0 20 40 60 80
Expression (TPM)
Expression (TPM)
Expression (TPM)
Expression (TPM)
Expression (TPM)

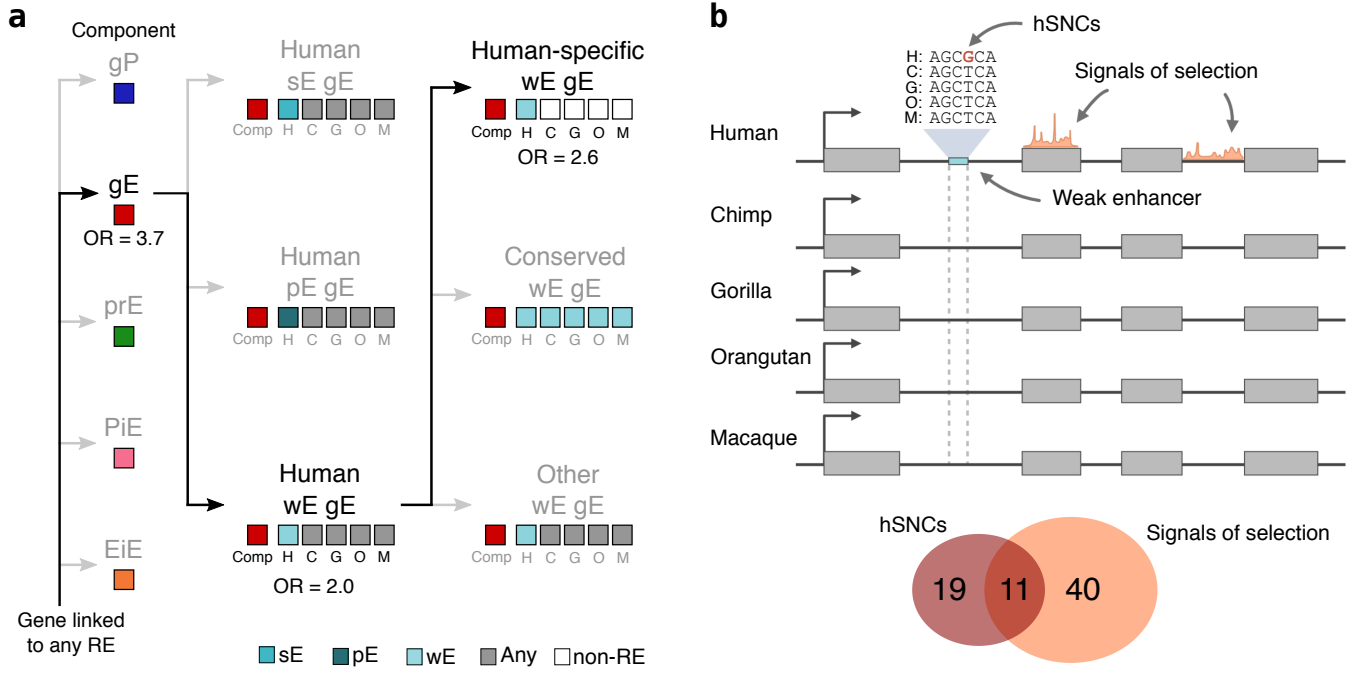
a
Component
gP
gE
OR = 3.7
prE
PiE
EiE
Gene linked to any RE
Human sE gE
Comp H C G O M
Human pE gE
Comp H C G O M
Human wE gE
Comp H C G O M
OR = 2.0
Human-specific wE gE
Comp H C G O M
OR = 2.6
Conserved wE gE
Comp H C G O M
Other wE gE
Comp H C G O M
sE
pE
wE
Any
non-RE
b
hSNCs
H: AGCGCA
C: AGCTCA
G: AGCTCA
O: AGCTCA
M: AGCTCA
Signals of selection
Weak enhancer
Human
Chimp
Gorilla
Orangutan
Macaque
hSNCs
Signals of selection
19
11
40